15. Dauer M, Obermaier B, Herten J, et al. Mature dendritic cells derived from human monocytes within 48 hours: a novel strategy for dendritic cell differentiation from blood precursors. J Immunol. 2003;170: 4069–4076.
16. Sporri R, Reis e Sousa C. Inflammatory mediators are insufficient for full dendritic cell activation and promote expansion of CD4+ T cell populations lacking helper function. Nat Immunol. 2005;6:163–170.
17. Langenkamp A, Messi M, Lanzavecchia A, Sallusto F. Kinetics of dendritic cell activation: impact on priming of TH1, TH2 and nonpolarized T cells. Nat Immunol. 2000;1:311–316.
18. Martin-Fontecha A, Sebastiani S, Hopken UE, et al. Regulation of dendritic cell migration to the draining lymph node: impact on T lymphocyte traffic and priming. J Exp Med. 2003;198:615–621.
19. Nair S, McLaughlin C, Weizer A, et al. Injection of immature dendritic cells into adjuvant-treated skin obviates the need for ex vivo maturation. J Immunol. 2003;171:6275–6282.
20. Berard F, Blanco P, Davoust J, et al. Cross-priming of naive CD8 T cells against melanoma antigens using dendritic cells loaded with killed allogeneic melanoma cells. J Exp Med. 2000;192:1535–1544.
21. Fujimoto T, Duda RB, Szilvasi A, Chen X, Mai M, O'Donnell MA. Streptococcal preparation OK-432 is a potent inducer of IL-12 and a T helper cell 1 dominant state. J Immunol. 1997;158:5619–5626.
22. Kitawaki T, Kadowaki N, Sugimoto N, et al. IgE-activated mast cells in combination with pro-inflammatory factors induce Th2-promoting dendritic cells. Int Immunol. 2006;18:1789–1799.
23. Nouri-Shirazi M, Banchereau J, Bell D, et al. Dendritic cells capture killed tumor cells and present their antigens to elicit tumor-specific immune responses. J Immunol. 2000;165:3797–3803.
24. Ohminami H, Yasukawa M, Fujita S. HLA class I-restricted lysis of leukemia cells by a CD8+ cytotoxic T-lymphocyte clone specific for WT1 peptide. Blood. 2000;95:286–293.
25. Kuzushima K, Hayashi N, Kudoh A, et al. Tetramer-assisted identification and characterization of epitopes recognized by HLA A*2402-restricted Epstein-Barr virus-specific CD8+ T cells. Blood. 2003; 101:1460–1468.
26. Vardiman JW, Harris NL, Brunning RD. The World Health Organization (WHO) classification of the myeloid neoplasms. Blood. 2002;100: 2292–2302.
27. Vardiman JW, Thiele J, Arber DA, et al. The 2008 revision of the World Health Organization (WHO) classification of myeloid neoplasms and acute leukemia: rationale and important changes. Blood. 2009;114:937–951.
28. Tsuboi A, Oka Y, Udaka K, et al. Enhanced induction of human WT1-specific cytotoxic T lymphocytes with a 9-mer WT1 peptide modified at HLA-A*2402-binding residues. Cancer Immunol Immunother. 2002;51:614–620.
29. Arai J, Yasukawa M, Ohminami H, Kakimoto M, Hasegawa A, Fujita S. Identification of human telomerase reverse transcriptase-derived peptides that induce HLA-A24-restricted antileukemia cytotoxic T lymphocytes. Blood. 2001;97:2903–2907.
30. Kuzushima K, Hayashi N, Kimura H, Tsurumi T. Efficient identification of HLA-A*2402-restricted cytomegalovirus-specific CD+ T-cell epitopes by a computer algorithm and an enzyme-linked immunospot assay. Blood. 2001;98:1872–1881.
31. Kokhaei P, Choudhury A, Mahdian R, et al. Apoptotic tumor cells are superior to tumor cell lysate, and tumor cell RNA in induction of autologous T cell response in B-CLL. Leukemia. 2004;18:1810–1815.
32. Ferlazzo G, Semino C, Spaggiari GM, Meta M, Mingari MC, Melioli G. Dendritic cells efficiently cross-prime HLA class I-restricted cytolytic T lymphocytes when pulsed with both apoptotic and necrotic cells but not with soluble cell-derived lysates. Int Immunol. 2000;12:1741–1747.
33. Hoffmann TK, Meidenbauer N, Dworacki G, Kanaya H, Whiteside TL. Generation of tumor-specific T lymphocytes by cross-priming with human dendritic cells ingesting apoptotic tumor cells. Cancer Res. 2000;60:3542–3549.
34. Galea-Lauri J, Wells JW, Darling D, Harrison P, Farzaneh F. Strategies for antigen choice and priming of dendritic cells influence the polarization and efficacy of antitumor T-cell responses in dendritic cell-based cancer vaccination. Cancer Immunol Immunother. 2004;53:963–977.
35. Spisek R, Chevallier P, Morineau N, et al. Induction of leukemia-specific cytotoxic response by cross-presentation of late-apoptotic leukemic blasts by autologous dendritic cells of nonleukemic origin. Cancer Res. 2002;62:2861–2868.
36. Itoh T, Ueda Y, Okugawa K, et al. Streptococcal preparation OK432 promotes functional maturation of human monocyte-derived dendritic cells. Cancer Immunol Immunother. 2003;52:207–214.
37. Kuroki H, Morisaki T, Matsumoto K, et al. Streptococcal preparation OK-432: a new maturation factor of monocyte-derived dendritic cells for clinical use. Cancer Immunol Immunother. 2003;52:561–568.
38. Okamoto M, Furuichi S, Nishioka Y, et al. Expression of Toll-like receptor 4 on Dendritic cells is significant for anticancer effect of dendritic cell-based immunotherapy in combination with an active component of OK-432, a streptococcal preparation. Cancer Res. 2004;64:5461–5470.
39. Nakahara S, Tsunoda T, Baba T, Asabe S, Tahara H. Dendritic cells stimulated with a bacterial product, OK-432, efficiently induce cytotoxic T lymphocytes specific to tumor rejection peptide. Cancer Res. 2003;63:4112–4118.
40. Dohnal AM, Graffi S, Witt V, et al. Comparative evaluation of techniques for the manufacturing of dendritic cell-based cancer vaccines. J Cell Mol Med. 2009;13:125–135.
41. Felzmann T, Huttner KG, Breuer SK, et al. Semi-mature IL-12 secreting dendritic cells present exogenous antigen to trigger cytolytic immune responses. Cancer Immunol Immunother. 2005;54:769–780.
42. Dohnal A, Witt V, Hügel H, Holter W, Gadner H, Felzmann T. Phase I study of tumor Ag-loaded IL-12 secreting semi-mature DC for the treatment of pediatric cancer. Cytotherapy. 2007;9:755–770.
43. de Vries IJM, Krooshoop DJEB, Scharenborg NM, et al. Effective migration of antigen-pulsed dendritic cells to lymph nodes in melanoma patients is determined by their maturation state. Cancer Res. 2003;63:12–17.
44. Morse MA, Coleman RE, Akabani G, Niehaus N, Coleman D, Lyerly HK. Migration of human dendritic cells after injection in patients with metastatic malignancies. Cancer Res. 1999;59:56–58.

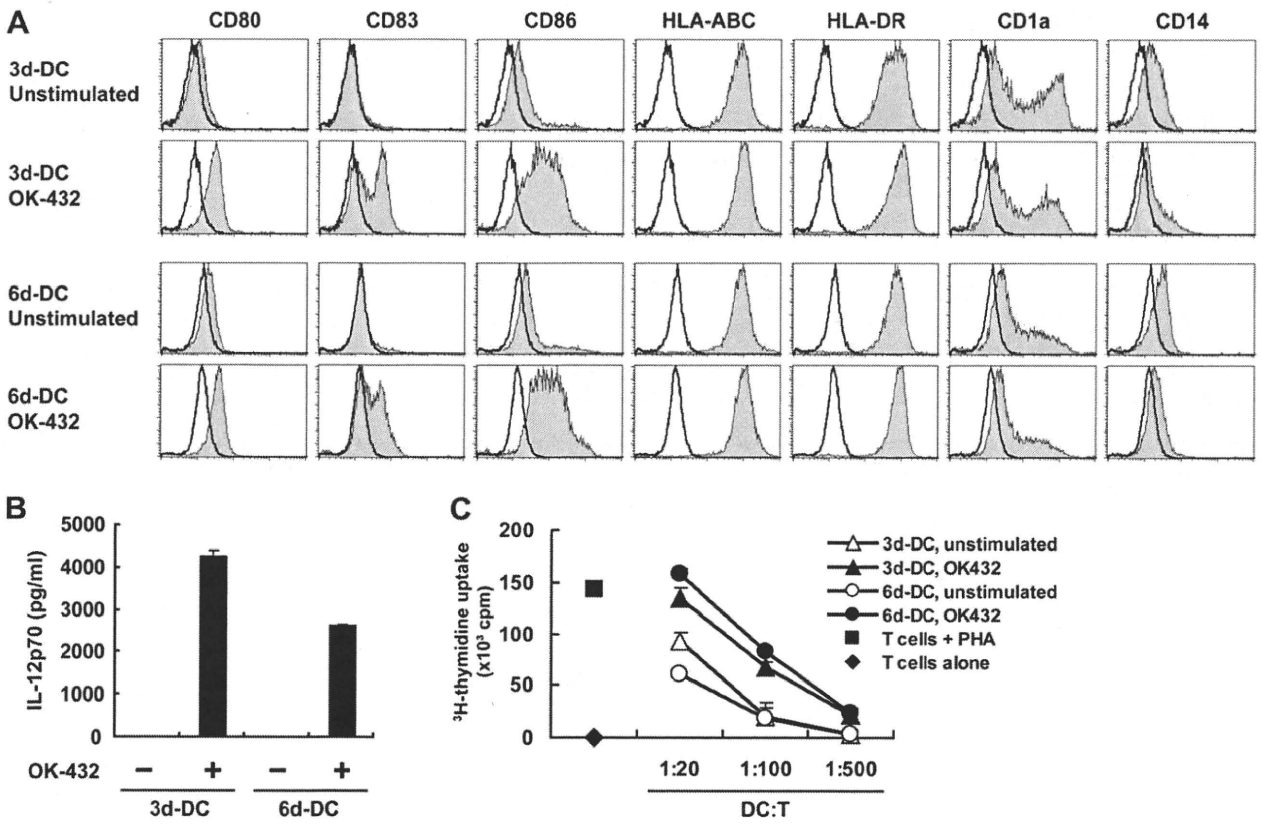

Supplementary Figure E1. 3d-DCs and 6d-DCs have comparable T-cell stimulatory capacity. (**A**) Expressions of surface molecules on DCs. Unstimulated or OK-432-stimulated DCs were analyzed by flow cytometry. Dead cells were excluded by staining with propidium iodide. Open histograms indicate staining with isotype controls. (**B**) IL-12p70 production by DCs (5×10^5 cells/mL) stimulated with OK-432 (0.1 KE/mL) for 24 hours was measured by enzyme-linked immunosorbent assay. Error bars indicate the standard deviation of duplicate measurements. (**C**) Proliferation of naive $CD4^+$ T cells stimulated with DCs. Allogeneic naive $CD4^+$ T cells were cocultured with DCs at indicated DC to T-cell ratios. On day 4, 1 Ci of [^{3}H]-thymidine was added. After 16 hours of further incubation, thymidine uptake was counted. Naive $CD4^+$ T cells were stimulated with 10 μg/mL phytohemagglutinin as a positive control. Representative data from three experiments are shown.

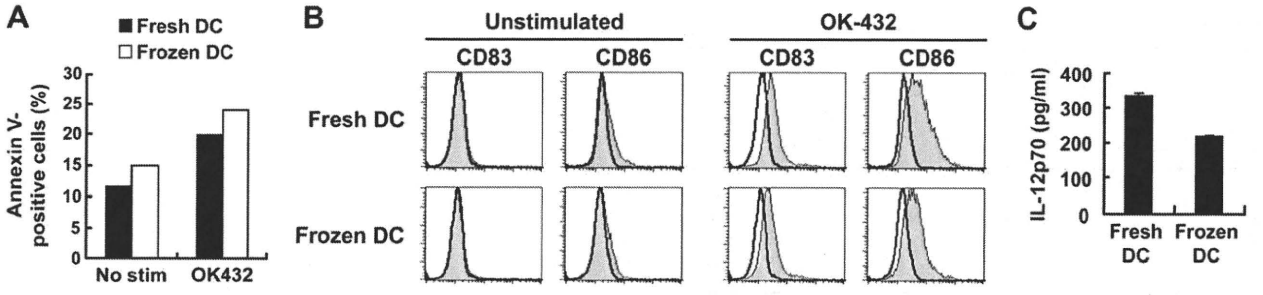

Supplementary Figure E2. Effects of cryopreservation on immature 3d-DCs. (**A**) Viability of fresh and frozen 3d-DCs after 24 hours of incubation with or without OK-432 (0.1 KE/mL) were evaluated by staining with Annexin-V. Percentages of Annexin-Vpositive cells are indicated. (**B**) Expression of surface molecules on fresh and frozen DCs after 24 hours of incubation with or without OK-432. (**C**) IL-12p70 production by fresh and frozen DCs (5×10^5 cells/mL) induced by 24-hour stimulation with OK-432 was measured by enzyme-linked immunosorbent assay. Error bars indicate the standard deviation of duplicate measurements. Representative data from four experiments are shown.

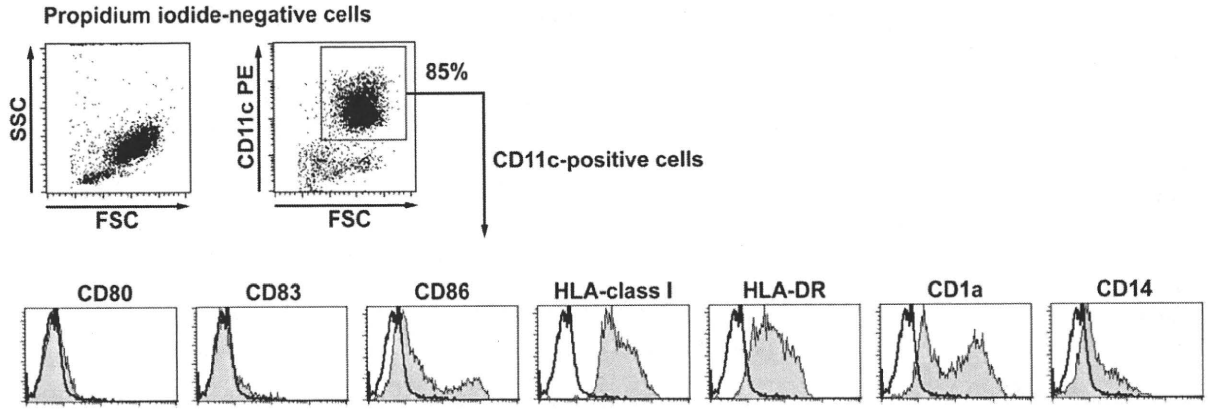

Supplementary Figure E3. Expression of surface molecules on DCs for vaccination. Cryopreserved DCs from patients were thawed, stained, and analyzed by flow cytometry. Dead cells were excluded by staining with propidium iodide. Numbers indicate percentages of cells in each quadrant. Representative data from patient no. 1 are shown.

Supplementary Table E1. DC vaccine generation

	At the time of apheresis				
Patient no.	Days after the last CT	PB WBC (/L)	PB Mo (%)	BM LC[a] (%)	Antigen dose (LC:DC)
1	74	4700	7	0.9	1:5
2	31	3000	9	2.0	1:6.5
3	43	3900	15	0[b]	1:6
4	46	4800	16	0.3	1:3.3

CT = chemotherapy; LC = leukemic cells; Mo = monocytes.
[a]Percentages of leukemic cells in bone marrow were determined by flow cytometry.
[b]Patient 3 was in complete remission at the time of apheresis. The patient subsequently relapsed and became eligible for DC vaccination.

第72回日本血液学会学術集会
教育講演
基本シリーズ S-7 骨髄異形成症候群

MDSの診断と分類；FAB分類からWHO分類へ

石川隆之

Key words : Myelodysplastic syndrome, WHO classification, FAB classification, Dysplasia

1. はじめに

骨髄異形成症候群（myelodysplastic syndrome; MDS）は，質的な異常を有する造血幹細胞のクローン性増殖に基づく疾患のうち，無効造血に伴う血球減少と血球形態異常を特徴とし，急性白血病に移行する危険が高いものと定義される。リンパ系腫瘍における遺伝子再構成のような明確な指標がないため，MDSにおいては，クローン性疾患であることの根拠を異形成所見で代用している。1982年にFrench-American-British（FAB）グループにより提唱されたMDSの分類（FAB分類，表1）は今だに輝きを失っていないいものの[1]，いくつかの問題点が指摘されるようになった。2001年にWHOよりMDSを含む造血器腫瘍の新たな分類（WHO分類2001）が提案された際，MDSの分類にも変更が加えられた[2]。WHO分類2001ではMDSと急性骨髄性白血病（acute myeloid leukemia; AML），骨髄増殖性疾患（myeloproliferative disorders; MPD）との境界を変更した以外に，非クローン性の血球減少症を排除する目的でMDSの診断に必要な条件を厳しくした。MDSと診断できない原因不明の血球減少症をどう扱うかなど，当初運用に戸惑いのあったWHO分類2001ではあるが，MDSの診断一致率を向上させること，MDS特異的な新規治療薬の治療対象の同定に役立つことなどが評価され，次第に受け入れられている。2008年のWHO分類改訂（WHO分類2008）では，WHO分類2001の考えを推し進めるとともに，論理的でわかりやすい分類とすることが意図された。一方，最近のMDSの発症ならびに進展に関する分子生物学的知見の集積は，WHO分類2008も過渡的なものであり，近い将来分子基盤に基づく画期的な分類の提案を予感させる。本稿では，WHO分類2008に至るまでの経過を記載することで，MDSの分類法の変更の必然性を記すとともに，今後の方向性についても考察したい。

京都大学大学院医学研究科 血液・腫瘍内科学

2. FAB分類

FAB分類（表1）はその簡便性が評価され，臨床試験の適格条件の設定などに現在もなお広く用いられている。しかし，FAB分類が多くの問題点を含むことも明らかになった[3]（表2）。

1）不応性貧血の診断に最低限必要な条件

Bennettらの FAB分類提唱の論文には，不応性貧血（refractory anemia; RA）の骨髄所見として「骨髄の細胞密度は正もしくは過形成で，赤芽球過形成または赤芽球の異形成を伴い，顆粒球系や巨核球系はほとんどの場合正常に見える」と記載されている。FAB分類では原因不明の血球減少があり，骨髄検査で強い異形成が見られない例でも，骨髄低形成でなければMDSと診断される傾向にあった。しかし骨髄の細胞密度は場所によって異なり，年齢にも左右され，少数回の骨髄検査で低形成ではないと断定することはできない。その結果，再生不良性貧血（再不貧）とFAB分類でのRAとの鑑別がしばしば問題となった。一方，異形成の存在はMDS診断の必須事項ではあるが，1990年代より異形成はMDSに限定されたものではなく，慢性炎症性疾患に伴う二次性の貧血，溶血発作，再不貧などにおいても赤芽球の異形成所見が認められることが知られるようになった。さらに，健常人骨髄標本を用いた検討でも，赤芽球の形態異常は稀ならず見られること[4]，高齢者では顆粒球や巨核球の形態異常も低頻度ながら認められることが報告された[5]。また，形態診断のエキスパート間においても，芽球比率と環状鉄芽球比率は一致率が高いが，異形成の判断の一致率は高くなかった[5]。異形成基準を明確にすることでの，異形成の診断一致率の向上は重要な問題で

表 1　FAB 分類

病型	定義	追加条件	1982 年当時の記載
refractory anemia（RA） 不応性貧血	1 と 2 を満たす　1. 末梢血の芽球 1％未満　2. 骨髄の芽球 5％未満	単球 1,000/μl 未満 環状鉄芽球 15％未満*	骨髄は正もしくは過形成，赤芽球系以外の異形成は稀
RA with ringed sideroblasts（RARS） 環状鉄芽球を伴う不応性貧血	1～3 をすべて満たす　1. 末梢血の芽球 1％未満　2. 骨髄の芽球 5％未満 3. 環状鉄芽球 15％以上*	単球 1,000/μl 未満	骨髄は正もしくは過形成，赤芽球系以外の異形成は稀
RA with excess blasts（RAEB） 芽球増加を伴う不応性貧血	1 または 2　1. 末梢血の芽球 5％未満で骨髄の芽球 5～19％　2. 末梢血の芽球 1～5％で骨髄の芽球 5％未満	単球 1,000/μl 未満 Auer 小体（－）	複数血球系統の減少と異形成がある
RAEB in transformation（RAEB-t） 移行期の芽球増加を伴う不応性貧血	1～3 のいずれか　1. 末梢血の芽球 5％以上　2. 骨髄の芽球 20～30％　3. 明瞭な Auer 小体を持つ		
chronic myelomonocytic leukemia（CMML） 慢性骨髄単球性白血病	1～3 のすべてを満たす　1. 単球 1,000/μl 以上　2. 末梢血の芽球 5％未満　3. 骨髄の芽球 20％未満	Auer 小体（－）	骨髄は RAEB に類似するが promonocyte の増加あり

＊環状鉄芽球は骨髄全有核細胞における比率

表 2　FAB 分類に関する論点（文献 3 より一部改変）

1. RA の診断に最低限必要な条件
2. RA/RARS の予後の多様性
3. 低形成 MDS
4. CMML は MDS か
5. RAEB. RAEB-t の予後の多様性
6. 染色体異常の扱い

あった。

2）不応性貧血/環状鉄芽球を伴う不応性貧血の予後の多様性

FAB 分類の RA は貧血と赤芽球の異形成を呈するものとされたが，赤芽球のみならず好中球や巨核球にも形態異常を示し，好中球減少，血小板減少を伴う患者も見られる。そのような例は予後不良染色体異常を持つ頻度が高く，白血病移行率が高く，生存期間が短い[6,7]。また，MDS の概念の提唱以前より，環状鉄芽球を呈するが赤芽球以外に形態異常を示さない「鉄芽球性貧血」は白血病移行を来しにくいことが知られていた。しかし，FAB 分類で環状鉄芽球を伴う不応性貧血（refractory anemia with ringed sideroblast; RARS）と診断されるもののなかには，好中球や巨核球の形態異常を示し，白血病移行率が高く生存期間が短い一群の患者が含まれる[8]。FAB 分類の RA，RARS は一般的に白血病移行に関しては低リスクとみなされるため，多系統の形態異常を伴う群を RA，RARS より分離することが望ましいと考えられるようになった。

3）低形成 MDS

1982 年の FAB 分類の提唱時には MDS は骨髄が正/過形成であると記載されたが，MDS の約 2 割で骨髄が低形成であること，低形成の例は高齢者に多いものの，それ以外の臨床像や予後との関連がないことが報告された[9]。骨髄が正/過形成であることはもはや MDS の必須条件ではないと考えられた。

4）慢性骨髄単球性白血病は MDS か

FAB 分類において慢性骨髄単球性白血病（chronic myelomonocytic leukemia; CMML）を MDS の 1 亜型とした根拠は，血球形態異常を伴うことと前白血病状態であることである。しかし，CMML は肝脾腫，胸水などの臓器腫大・臓器浸潤を高率に認め，しばしば高度の白血球増加を伴うなど，MPD としての性格を兼ね備えている。1994 年に FAB グループは白血球数 13,000 を指標として，それ以下のものを MDS 型 CMML，それ以上のものを MPD 型 CMML と呼ぶことを提唱したが[10]，

両者の病態に本質的な差がないとする報告もなされている[11]。

5) RAEB，RAEB-t の予後の多様性

芽球増加を伴う不応性貧血（RA with excess blasts; RAEB）や移行期の芽球増加を伴う不応性貧血（RAEB in transformation; RAEB-t）においても，骨髄の芽球比率は重要な予後因子であり，とくに骨髄の芽球比率 10%未満もしくは以上で生存期間が異なることが報告された[12, 13]。また，骨髄の芽球比率 20～30%のものは短期間で AML に移行する頻度が高く，*de novo* 発症の AML を一部含むことからも，AML とみなすべきとする考えもあった。RAEB-t には骨髄芽球比率が 20%未満ながら末梢血芽球比率 5%以上のものとアウエル小体により規定されるものが含まれるが，これらが骨髄の芽球比率で定義された RAEB-t と同等の予後を持つかも明らかでなかった[14, 15]。

6) 染色体異常の扱い

骨髄に多くの低分葉巨核球を認め，貧血を示すが血小板減少は稀で，長期間安定した経過を示し，女性に多く，染色体分析で 5q－単独の異常を呈するという特徴を示す血球減少症に対して，1975 年に既に 5q⁻症候群という名称が与えられていた[16, 17]。FAB 分類では RA もしくは RARS に含まれたが，白血病移行率が低く，生存期間も長いことから，疾患単位として独立させることが望ましいと考えられるようになった。

クローン性細胞増殖を示す染色体異常を呈するものの，明らかな形態異常を伴わない血球減少症が存在する。そのような例に対して従来は，骨髄が正もしくは過形成の場合 MDS と，骨髄低形成と汎血球減少を示す場合には再生不良性貧血と診断されてきた。最近の CGH アレイや SNP アレイ解析の進歩により，染色体分析では判明し得なかった遺伝子異常が明らかにされるようになったが[18]，最近では染色体異常や後天的な遺伝子異常を呈し，血球減少を認める例は，異形成の有無によらず MDS と診断するべきでないかと考える研究者が多い。

3. WHO 分類

2001 年に公表された WHO 分類（WHO 分類 2001）は造血器腫瘍を網羅したものであり，悪性リンパ腫では免疫染色の解析結果が診断に取り入れられ，慢性骨髄性白血病や AML では染色体や遺伝子の情報が分類の決め手にされた。一方，MDS の分類は形態学に依存している点で基本的には FAB 分類を踏襲したものであった。WHO 分類 2001 の大きな特徴は，非クローン性の反応性病態を MDS から排除することを目的に，異形成を示す細胞が一定の比率で認められることを MDS と診断するための前提条件としたことである。その後，2008 年の WHO 分類の改訂（WHO 分類 2008）にあたり，芽球増加を示さない MDS の分類をより明確にするための修正がなされた（表 3）。

1) MDS 診断の必須項目

WHO 分類 2001 では血球系列ごとに異形成の定義を行い，芽球増加を示さない例においては，おのおのの血球系列で 10%以上の細胞（環状鉄芽球は赤芽球の 15%）にいずれかの異形成所見が見られるときのみ MDS の診断がなされることとした（表 4）。また，異形成が見られたとしても特に芽球増加を伴わない際には，病歴などにより反応性の血球減少症を十分に除外する必要があると記載されている（表 5）。WHO 分類 2008 年では，異形成の判断には赤芽球系ならびに好中球系はそれぞれ 200 個，巨核球は 30 個の細胞を観察する必要があると明記された。二次性貧血や健常人の骨髄標本の検討から，MDS 診断に必要な異形成細胞比率の閾値を巨核球系においては 40%に高めるべきであるという意見もある[19]。

MDS の診断を厳しくしたことで，他に原因を求められない持続する血球減少があり，一部の血球に異形性を認めるもののその比率が 10%を超えず，MDS と診断できない例をどのように扱うかが問題となった。2006 年の Working Conference on MDS において，異形成を示す細胞比率が 10%未満であっても，MDS に特徴的な染色体異常や，クローン性疾患であることを示す証拠が得られた場合は，MDS を強く疑う病態とみなすことが提案された。また，表 6 の A の血球減少の基準を 6 ヶ月以上継続して満たし，他の疾患が除外されるが，B，C の基準を満たさない例を，MDS への移行を含めて注意深い経過観察が望まれる病態として，特発性血球減少症（idiopathic cytopenia with unknown significance; ICUS）と命名することも提案された[20]。WHO 分類 2008 では Working Conference での提唱を一部取り入れ，血球減少と特徴的な染色体異常（Working Conference で認められた＋8，－Y，del20q 単独の異常は WHO 分類 2008 では除外されている）がありながら，芽球増加も有意な異形成所見も見られない例を分類不能型 MDS（MDS, unclassifiable; MDS-U）に含めることとされた。また，ICUS の考えも記載されている。ただし，血球減少の定義は IPSS を踏襲して，Hb 10 g/*dl* 未満，好中球 1,800/*μl* 未満，血小板 10 万/*μl* 未満としている。

2) FAB 分類における RA/RARS

FAB 分類における RA は白血病移行の危険性や生存期間において均質な集団ではなかった。均質な予後を持つ疾患群への再分類のため，2001 年の WHO 分類では 5q-症候群を取り出したほか，赤芽球のみの異形成を示す RA，好中球もしくは巨核球のみの異形成を示す MDS-U

表3 WHO 分類による MDS

WHO 分類 2008	WHO 分類 2001	FAB 分類
1 系統に異形成を伴う不応性血球減少症 (refractory cytopenia with unilineage dysplasia, RCUD) #1		
不応性貧血（RA）	不応性貧血 refractory anemia（RA）	不応性貧血（RA）
不応性好中球減少症 (refractory neutropenia, RN)	分類不能型 MDS（MDS-U）#2	
不応性血小板減少症 (refractory thrombocytopenia, RT)	分類不能型 MDS（MDS-U）#2	
多血球系異形成を伴う不応性血球減少症 (refractory cytopenia with multilineage dysplasia, RCMD)	多血球系異形成を伴う不応性血球減少症（RCMD）	不応性貧血（RA）
	環状鉄芽球と多血球系異形成を伴う不応性血球減少症（RCMD-RS）	環状鉄芽球を伴う不応性貧血 (RARS)
環状鉄芽球を伴う不応性貧血（RARS）#3	環状鉄芽球を伴う不応性貧血 (RARS) #3	環状鉄芽球を伴う不応性貧血 (RARS) #4
染色体異常 isolated del（5q）を伴う MDS（MDS with isolated del（5q））	染色体異常 isolated del（5q）を伴う MDS（MDS with isolated del（5q））	不応性貧血（RA）もしくは環状鉄芽球を伴う不応性貧血（RARS）
分類不能型 MDS (MDS, unclassifiable, MDS-U) #5	該当するものなし	不応性貧血（RA）もしくは環状鉄芽球を伴う不応性貧血（RARS）もしくは芽球増加を伴う不応性貧血 (RAEB)
芽球増加を伴う不応性貧血（RAEB）	芽球増加を伴う不応性貧血 (RAEB)	
RAEB-1 #6	RAEB-1 #6	芽球増加を伴う不応性貧血 (RAEB)
RAEB-2 #7	RAEB-2 #8	芽球増加を伴う不応性貧血 (RAEB）もしくは移行期の芽球増加を伴う不応性貧血（RAEB-t）#9

#1 血球減少は 1 もしくは 2 系統で，血球減少を認めないもの，汎血球減少を示すものは含まない。異形成を認める血球系列によって以下の 3 つに分類する。
#2 WHO 分類 2008 における分類不能型 MDS とは全く別の概念
#3 環状鉄芽球は赤芽球の 15%以上
#4 環状鉄芽球は骨髄全有核細胞の 15%以上
#5 1)～3）のいずれかを満たすもの。1）RCUD もしくは RCMD に該当し，末梢血に 1%の芽球を認める　2）1 系統に異形成を認め，汎血球減少を呈する　3）芽球増加がなく異形成所見も明らかでないが，MDS が推定される染色体異常がある
#6 1)，2）のいずれかを満たし，単球増加とアウエル小体を認めないもの。1）骨髄の芽球比率 5～9%かつ末梢血の芽球比率 5%未満　2）末梢血の芽球比率が 2%～ 5%かつ骨髄の芽球比率 10%未満
#7 1)～3）のいずれかを満たし，単球増加を認めないもの。1）骨髄の芽球比率 10～19%かつ末梢血の芽球比率 19%未満　2）骨髄の芽球比率 19%未満かつ末梢血の芽球比率 5～19%　3）芽球比率は RCMD，MDS-U，RAEB-1 であるがアウエル小体を認める
#8 1)～3）のいずれかを満たし，単球増加を認めないもの。1）骨髄の芽球比率 10～19%かつ末梢血の芽球比率 19%未満　2）骨髄の芽球比率 19%未満かつ末梢血の芽球比率 5～19%　3）芽球比率は RAEB-1 であるがアウエル小体を認める
#9 RAEB-t のうち，末梢血芽球比率 5%ｉ以上で骨髄芽球比率 20%未満のものと，アウエル小体を持つものが RAEB-2 に該当

表 4　FAB 分類と WHO 分類の比較

			FAB 分類 1982	WHO 分類 2001	WHO 分類 2008
血球減少			記載なし	記載なし	Hb＜10 g/dl，好中球＜1,800/μl，血小板＜10 万/μl
骨髄細胞密度			正もしくは過形成	正もしくは過形成だが一部では低形成	多くは正もしくは過形成だが，10%程度低形成の例がある
芽球			promonocyte, proerythroblast, megakaryoblast は含めない	記載なし	monoblast, promonocyte, megakaryoblast を含める
			核が偏在したもの，ゴルジ野の発達したもの，核クロマチンが凝集したもの，アズール顆粒を多数持つもの，N/C 比が低いもの，は含めない		
異形成	赤芽球	核	multinuclearity, nuclear fragments, abnormal nuclear shape	budding, internuclear bridging, karyorrhexis, multinuclearity, megaloblastic change	
		細胞質	ringed sideroblast, abnormal cytoplasmic feature	ring sideroblast, vacuolisation, PAS positivity	
		頻度	記載なし	10%以上	
	顆粒球	核	hyposegmentation, hypersegmentation	hypolobulation, hypersegmentation	
		細胞質	a- or hypo-granular, cytoplasmic basophilia in mature cells, large primary granules	hypogranularity, pseudo Chediak-Higashi granules	
		大きさ		small size	
		頻度	記載なし	10%以上	
	巨核球	核	large mononuclear, multiple small separated nuclei	non-lobulated, multiple and widely-separated nuclei	
		全体像	micromegakaryocyte	hypolobulated micromegakaryocyte	
		頻度	記載なし	10%以上	

(WHO 分類 2008 の MDS-U とはまったく異なる概念であることに注意)，多系統の異形成をもつ多血球系異形成を伴う不応性血球減少症（refractory cytopenia with multilineage dysplasia; RCMD）と異形成を示す血球系列，系列数により分類した。RARS も赤芽球のみの異形成を示す RARS と，赤芽球以外の血球系統にも異形成を示す環状鉄芽球と多血球系異形成を伴う不応性血球減少症（RCMD-RS）に分類された。RCMD，RCMD-RS という予後不良例を除外することで，RA と RARS を白血病移行の危険の低い集団として独立させたものであるが，その後の検証によっても RA，RARS，5q－症候群の予後は良好である一方，RCMD，RCMD-RS は白血病移行率が高く有意に予後不良であることが確認された[21]。

WHO 分類 2008 では，WHO 分類 2001 の RA と MDS-U を 1 系統に異形成を伴う不応性血球減少症（refractory cytopenia with unilineage dysplasia; RCUD）としてまとめ，その中に RA，不応性血小板減少症（refractory thrombocytopenia; RT），不応性好中球減少症（refractory neutropenia; RN）というサブカテゴリーをおいた。RA と RARS はともに異形成が赤芽球系に限局しているものの，歴史的な背景などから独立した疾患単位と考えられているが，WHO 分類 2001 において記載された RCMD と RCMD-RS は予後に違いが見られなかったことから RCMD に統一された。血球減少と MDS に特徴的な染色体異常を持つものの形態異常に乏しいものや，骨髄は RCUD もしくは RCMD であるが末梢血に 1%の芽球を認めるもの，さらに単一血球系統に異形成を示すが汎血球減少を示すものは，慎重に病型移行を観察する必要があることから，MDS-U としてまとめられた。MDS 分類 2001 でもそうであったが，MDS-U はその段階で適当な位置づけの不明な病態に対して暫定的につけられた名称である。

表 5 MDS と鑑別を要する二次性血球減少症

ビタミン B12 もしくは葉酸欠乏症*
重金属中毒（特にヒ素）*
先天性血液異常症*
パルボウイルス感染症*
薬剤使用（化学療法薬，G-CSF など）*
発作性夜間血色素尿症*
慢性疾患に伴う貧血
自己免疫性疾患（慢性関節リウマチ，SLE，炎症性腸疾患など）
感染症（結核，HIV など）
他の悪性腫瘍
腎性貧血
慢性肝疾患
アルコール過剰摂取

＊WHO 分類で言及されているもの

3) FAB 分類における RAEB ならびに RAEB-t

IPSS で採用された骨髄芽球比率 10%の予後に与える影響を踏襲し，骨髄の芽球比率 10%未満のものを RAEB-1，10～19%のものを RAEB-2 とした。一方，末梢血芽球比率は RAEB-1 では 5%未満であり，末梢血で 5～19%の芽球をもつものは RAEB-2 に含まれる。WHO 分類 2001 ではアウエル小体の持つ意義は不明としつつも，RAEB の基準を満たしつつアウエル小体を持つもの

表 6 Working Conference on MDS で提案された MDS 診断の必須項目#1（文献 20）

(A) 必須基準（1），2）をともに満たすこと）
1) 1 系統以上の血球減少
Hb 11 g/dl 未満，好中球 1,500/μl 未満，血小板 10 万/μl 未満
2) 血球減少や異形性の原因となるを他の造血系/非造血系疾患の除外#2
(B) MDS 関連（決定的）基準（(1)-3）のいずれかを満たす必要あり）
1) 骨髄スメアの検鏡で，赤芽球，好中球，巨核球のうち 1 つの細胞系列で 10%以上の細胞に異形成を認めるか，鉄染色で 15%以上の赤芽球に環状鉄芽球を認める
2) 骨髄スメア標本に 5～19%の芽球を認める
3) 通常の染色体検査もしくは FISH 法で典型的な染色体異常が見られる#3
(C) 補助基準#4（A を満たすが B を満たさないものの，輸血依存性の大球性貧血など典型的な MDS の症状を示すとき，以下のいずれかを満たせば MDS の可能性が極めて高い）
1) フローサイトメトリー法により，赤芽球系もしくは好中球系の細胞に単クローン性集団が存在することを示唆する異常な表現型が示されること
2) HUMARA 法，gene chip profiling，点突然変異（例えば RAS 変異）により，分子生物学的に単クローン性集団が示される
3) 骨髄もしくは末梢血造血前駆細胞が著しくかつ持続的なコロニー形成の低下を示す（CFU-assay）

#1 必須基準と決定的基準の少なくとも一つが満たされたとき MDS と診断できる。決定的基準を満たさないが，クローン性血液疾患である可能性が高い際には補助基準を検討する。補助基準は MDS もしくは MDS を強く疑う状態との結論を得る上で役立つであろう。
#2 他に血球減少をきたしうる疾患があっても，MDS と診断できる場合がある
#3 典型的な染色体異常は＋8，－7，5q－，20q－，その他である。染色体異常のみ MDS 関連基準を満たす場合，MDS を強く疑う状態とみなすべきである。
#4 補助基準はすべての施設で可能な通常の検査項目ではない。基準を当てはめることができなければ，経過観察により MDS の診断を確かなものとするべきである。

はRAEB-2に診断することとしたが，アウエル小体の存在は白血病移行の危険を高めるという報告により[22]，WHO分類2008では，芽球比率によらず（RCMDに該当する例でも）アウエル小体があればRAEB-2と診断することとされた。MDS患者の少なからぬ割合で骨髄のreticulin線維増生をきたすが，そのような例では質の高い骨髄スメア標本が得られず，異形成や芽球比率の評価が困難である。また，骨髄の線維化を伴うAMLや原発性骨髄線維症のみならず，HIV感染症や自己免疫性疾患で見られる反応性の骨髄線維化との鑑別も問題になる[23]。WHO分類2008では，骨髄生検標本を用いたCD34の免疫染色などにより芽球比率を算定することが勧められ，RAEBに合致する芽球比率が得られるとともに，二系統以上の異形成が認められればRAEB with fibrosis（RAEB-F）とすることが提唱された。

末梢血もしくは骨髄での芽球比率が20%を超えたものはWHO分類ではAML with multilineage dysplasia (2001) もしくはAML with myelodysplasia -related changes (2008) に分類される。骨髄の芽球比率が20～30%のFAB分類でのRAEB-tと，芽球比率30%以上のAML with multilineage dysplasiaで生存期間が違わなかったとの報告もあり[24]，WHO分類によるAMLの定義の変化はおおむね受け入れられている。

4) FAB分類におけるCMML

CMMLは形態的異形成と無効造血を呈するが，末梢血で単球のみならず時に顆粒球の増加を伴うことから，WHO分類2001においてはmyelodysplastic/myeloproliferative disease (MDS/MPD) というMDSやMPDとことなる新たな疾患カテゴリーに移された。WHO分類2001におけるCMMLの定義は末梢血における持続的な単球増多（1,000/μl以上），bcr/abl融合遺伝子の欠如，末梢血および骨髄の芽球（＋前単球）比率20%以下，異形成を示す血球系列があることと定められ，その上で，RAEB-1，-2と同じく，末梢血と骨髄の芽球比率に応じてCMML-1とCMML-2に分けることが提案された。WHO分類2008では，診断基準に好酸球増加を伴う場合にPDGFRAとPDGFRBの再構成を伴っていないことを確認する必要がある，という文章が追加されたが，それ以外の訂正はなされていない。Azacytidineなどの脱メチル化薬はRAEBとともにCMMLにも奏効すること[25]，FAB分類での全例を対象とした後方視的解析によりCMMLであることは単変量でも多変量でも予後に影響を与える因子でなかったこと[26]などから，CMMLをMDSから除外することに異論もあるが，CMMLは同じくMDS/MPD（MPN）に分類される若年性骨髄単球性白血病（juvenile myelomonocytic leukemia; JMML）と形態的に類似するのみならず，分子基盤も重複していたことが示されたが，このことは[27]，MDS/MPD（MPN）カテゴリー新設の妥当性を示すものである。

4. MDSの形態学的異形成に基づく診断確度区分（特発性造血障害に関する調査研究班）

WHO分類2001の提唱と2005年のMDSの形態診断標準化を目指す国際ワーキンググループ（International Working Group on MDS morphology; IWG-MDS）の結成を受け，IWG-MDSでまとめられた異形成に関するコンセンサスを日本で普及させることを目的に，松田らによってMDSの形態学的異形成に基づく診断確度区分が作成された（表7）。WHO分類で記載された異形成のなかにも，炎症や造血刺激などにより反応性に起こりうるものと，MDSに特異性の高いものがあることが知られている。具体的には，偽ペルゲル核異常好中球，無もしくは低顆粒好中球，微小巨核球，環状鉄芽球の4つはMDSに特異性が高いが（カテゴリーAの異形成），それ以外（カテゴリーBの異形成）は反応性の病態でもしばしば観察される。他に原因を求められない血球減少症で，カテゴリーAの異形成を高頻度に認めればMDSの診断は確定的であるが，カテゴリーBの異形成を1血球系統にのみ認める例ではMDSの可能性はあるが断定困難である。診断確度区分とは，芽球比率，異形成の程度，染色体所見を総合して，MDSと診断されるものおよびその可能性があるものを診断確度に応じてdefinite，probable，possibleの3つに区分したものである。原因不明の血球減少症で確度区分がpossibleにもならないものはICUSとする。ICUSのみならずMDS possibleにも種々の非MDS例の混入が予想されることから，そのような例は当面脱メチル化薬などMDSに対する特異的な治療の対象とせず経過観察することが推奨される。臨床的に鑑別が最も難しいMDSと再生不良性貧血の診断に関しては，まず骨髄生検を含む複数箇所の骨髄検査と脊椎骨MRIにより骨髄細胞密度の評価を行い，骨髄が低形成の場合，MDSを積極的に支持する所見（明確な異形成か高率の染色体異常）がなければ再生不良性貧血と診断することとしている。

5. 形態によらないMDS診断の試み

FAB分類もWHO分類も形態を診断の基本にしており，異形成の評価は現時点でMDSの診断には欠かせない。しかし，正確で信頼性の高い形態診断のためには，末梢血混入の少ない骨髄検体の採取，良好な塗末標本の作成，質の高い染色のすべてを満たすことが必要である。また，骨髄低形成の場合，WHO分類2008で推奨される数の血球数の観察は容易でない。異形成の定義を

表7 MDSの形態学的異形成に基づく診断確度区分（特発性造血障害に関する調査研究班）

(A) MDS診断のための必要条件
以下のすべてを満たす
1) 1系統以上の持続する血球減少
Hb＜11 g/dl
好中球＜1,500/μl
血小板＜10万/μl
2) 末梢血と骨髄の芽球比率20%未満で以下の染色体異常がない
t(8;21)(q22;q22), t(15;17)(q22;q12), inv(16)(p13;q22), t(16;16)(p13;q22)
3) 末梢血の単球数が1,000/μl未満
4) 血球減少の原因となる他の血液疾患および非血液疾患の除外
5) 再生不良性貧血の除外
骨髄が低形成の場合に，形態学的所見と染色体所見を参考に検討

(B) 定量的判定に基づく異形成の程度の区分
High 1) もしくは2) を満たすもの
1) Pelgerまたは Hypo-Gr 10%以上かつ mMgk 10%以上
2) 環状鉄芽球が赤芽球の15%以上
Intermediate
2-3系統で異形成＃10%以上
Low
1系統で異形成＃10%以上
Minimal
1-3系統で異形成＃1～9%

Pelger: 偽ペルゲル核異常好中球 Hypo-Gr; 無/低顆粒好中球 mMgk; 微小巨核球
＃WHO 2001に記載されたすべての異形成所見を含む

(C) 診断確度区分

診断確度区分	骨髄芽球比率(%)	異形成の程度区分	染色体所見*
MDS definite	5～19	High, Int., Low	Any
	0～4	High, Int., Low	Abnormal
	0～4	High	Any
MDS probable	0～4	Int	Normal or Unknown
MDS possible	0～4	Low	Normal or Unknown
ICUS	0～4	Minimal	Normal or Unknown

＊5q－, －7/7q－, ＋8, 20q－, complex, others

定めたとはいえ，RCUDとRCMDの鑑別に迷う例は少なくない。近年，Working Conference on MDSの報告で示されたようにMDSの診断に染色体検査のみならず，フローサイトメトリー（Flowcytometry; FCM）や遺伝子検査を用いることが模索されている（表6）。

1) フローサイトメトリー

内在する遺伝子異常の結果生じる表面抗原発現の変化や血液細胞の異形成をFCMにより検出し，MDSの診断，さらには予後の層別化にも用いることは以前より試みられてきた[28]。すなわち，好中球，赤芽球もしくは単球の異常は，膜抗原発現の異常（減弱，増強，異所性発現）を伴うことが多く，好中球の脱顆粒はFCMでの側方散乱光（side scatter; SSC）の低下に反映される。骨髄塗抹標本での芽球はFCMではおおむね$CD45^{dim}SSC^{low}CD34^{+}$の分画に相当するものの，FCMに用いられるサンプルには塗末標本以上に末梢血の混入が避けられないこと，CD34抗原を発現しない芽球がしばしば見られることなどから，FCMは芽球比率の算定には向か

ない。しかし，多重染色法を用いることで，低頻度であってもクローン性の骨髄芽球もしくは赤芽球集団を検出でき，異常細胞の質的評価から予後予測まで可能であるといわれている[29~31]。2008年のEuropean LeukemiaNet (ELN) ワークショップで，FCMの標準化（細胞の処理方法，染色法，検索に用いる最低限の抗体の組み合わせなど）に関する提言がなされ，今後前方視的検討を進めていくことが確認された[32]。診断確度区分でICUS, MDS possible, MDS probableとされる例を中心として，今後FCMが信頼性の高い補助診断法となることが期待される。

2）遺伝子解析

AMLでは多くの均衡型転座による染色体異常が知られ，融合遺伝子の解析から病型分類にも用いられているが，MDSでは不均衡型転座や染色体のモノソミー，部分欠失などの結果生じる数的異常が多く，MDSの発症や進展に関連する遺伝子の同定は遅れていた。近年single nucleotide polymorphisms (SNP) アレイを用いることで遺伝子の数的変化が詳細かつ正確に判明するようになり，特に染色体分析では判明し得ないuniparental disomy (UPD) といわれる片親由来の遺伝子重複を伴うヘテロ性の喪失現象を高頻度に認めることが報告された[18,33]。SNPアレイで得られた遺伝子異常に関する情報は，MDSの有力な補助診断法となるだけでなく，予後予測にも用いられるであろう。

以前よりMDSにはRUNX1，RASなどの遺伝子変異が知られていたが，それらの変異はアルキル化剤投与後の二次性MDSや芽球の増加した進行病期に多く，*de novo* のRA/RCMDではまれであった[34]。最近UPD領域に重要な遺伝子変異が存在することが知られるようになり[35]，変異遺伝子が知られていなかったUPD領域からTET2やCbl変異が新たに報告された[27,36]。TET2変異は*de novo* MDSの約2割で見られるほか，MPD/MPNやAMLにおいても確認されている。また，TET2変異陽性のMDSは比較的予後良好という報告もあり，今後病型分類に用いられる可能性がある[37]。現在進行中のゲノム解析技術の進歩は，MDSの発症や進展に関連した多くの新規変異遺伝子を同定するかもしれない[38]。それにより，MDSの分子病態の解明のみならず，形態に依存してきた診断や分類法に変化をもたらす可能性がある。

6. 結　語

FAB分類はAML，ALL，MDSのいずれにおいても形態に基づくものであった。WHO分類になり，AMLやALLでは予後の推定や治療法の選択に有用であることから，細胞膜抗原解析や遺伝子解析が重視されるようになった。MDSは発症，進展に多くの遺伝子異常の関与が考えられ，一つの遺伝子異常のもつ意味はAMLやALLほど大きくないと予想される。しかし，骨髄系腫瘍の枠組みの見直しを含めて，遺伝子変異はいずれ何らかの形でMDSの分類にも反映されると思われる。一方，レナリドマイドや脱メチル化薬の登場はMDSの自然経過に影響を及ぼし，新たな予後良好群を生み出すことが期待される。今後は治療反応性を包含した分類の作成も求められるであろう。

文　献

1) Bennett JM, Daniel MT, Flandrin G, et al. Proposals for the classification of the myelodysplastic syndromes. Br J Haematol. 1982; **51**: 189-199.
2) Harris NL, Jaffe ES, Diebold J, et al. World Health Organization classification of neoplastic diseases of the hematopoietic and lymphoid tissues: report of the Clinical Advisory Committee meeting-Airlie House, Virginia, November 1997. J Clin Oncol. 1999; **17**: 3835-3849.
3) Germing U, Gattermann N, Strupp C, Aivado M, Aul C. Validation of the WHO proposals for a new classification of primary myelodysplastic syndromes: a retrospective analysis of 1600 patients. Leuk Res. 2000; **24**: 983-992.
4) Bain BJ. The bone marrow aspirate of healthy subjects. Br J Haematol. 1996; **94**: 206-209.
5) Ramos F, Fernández-Ferrero S, et al. Myelodysplastic syndrome: a search for minimal diagnostic criteria. Leuk Res. 1999; **23**: 283-290.
6) Rosati S, Mick R, Xu F, et al. Refractory cytopenia with multilineage dysplasia: further characterization of an 'unclassifiable' myelodysplastic syndrome. Leukemia. 1996; **10**: 20-26.
7) Matsuda A, Jinnai I, Yagasaki F, et al. Refractory anemia with severe dysplasia: clinical significance of morphological features in refractory anemia. Leukemia. 1998; **12**: 482-485.
8) Gattermann N, Aul C, SchneiderW. Two types of acquired idiopathic sideroblastic anaemia (AISA). Br J Haematol. 1990; **74**: 45-52.
9) Tuzuner N, Cox C, Rowe JM, Watrous D, Bennett JM. Hypocellular myelodysplastic syndromes (MDS): new proposals. Br J Haematol. 1995; **91**: 612-617.
10) Bennett JM, Catovsky D, Daniel MT, et al. The chronic myeloid leukaemias: guidelines for distinguishing chronic granulocytic, atypical chronic myeloid, and chronic myelomonocytic leukaemia. Proposals by the French-American-British Cooperative Leukaemia Group. Br J Haematol. 1994; **87**: 746-754.
11) Germing U, Gattermann N, Minning H, Heyll A, Aul C. Problems in the classification of CMML—dysplastic versus proliferative type. Leuk Res. 1998; **22**: 871-878.
12) Sanz GF, Sanz MA, Vallespí T, Two regression models and a

scoring system for predicting survival and planning treatment in myelodysplastic syndromes: a multivariate analysis of prognostic factors in 370 patients. Blood. 1989; **74**: 395-408.

13) Greenberg P, Cox C, LeBeau MM, et al. International scoring system for evaluating prognosis in myelodysplastic syndromes. Blood. 1997; **89**: 2079-2088.
14) Seymour JF, Estey EH. The prognostic significance of auer rods in myelodysplasia. Br J Haematol. 1993; **85**: 67-76.
15) Strupp C, Gattermann N, Giagounidis A, et al. Refractory anemia with excess of blasts in transformation: analysis of reclassification according to the WHO proposals. Leuk Res. 2003; **27**: 397-404.
16) Sokal G, Michaux JL, Van Den Berghe H, et al. A new hematologic syndrome with a distinct karyotype: the 5 q-- chromosome. Blood. 1975; **46**: 519-533.
17) Boultwood J, Lewis S, Wainscoat JS. Wainscoat, The 5q- syndrome. Blood. 1994; **84**: 3253-3260.
18) Gondek LP, Tiu R, O'Keefe CL, Sekeres MA, Theil KS, Maciejewski JP. Chromosomal lesions and uniparental disomy detected by SNP arrays in MDS, MDS/MPD, and MDS-derived AML. Blood. 2008; **111**: 1534-1542.
19) Matsuda A, Germing U, Jinnai I, et al. Improvement of criteria for refractory cytopenia with multilineage dysplasia according to the WHO classification based on prognostic significance of morphological features in patients with refractory anemia according to the FAB classification. Leukemia. 2007; **21**: 678-686.
20) Valent P, Horny HP, Bennett JM, et al. Definitions and standards in the diagnosis and treatment of the myelodysplastic syndromes: Consensus statements and report from a working conference. Leuk Res. 2007; **31**: 727-736.
21) Germing U, Strupp C, Kuendgen A, et al. Prospective validation of the WHO proposals for the classification of myelodysplastic syndromes. Haematologica. 2006; **91**: 1596-1604.
22) Germing U, Strupp C, Kuendgen A, et al. Refractory anaemia with excess of blasts (RAEB): analysis of reclassification according to the WHO proposals. Br J Haematol. 2006; **132**: 162-167.
23) Vardiman JW. Hematopathological concepts and controversies in the diagnosis and classification of myelodysplastic syndromes. Hematology Am Soc Hematol Educ Program. 2006; 199-204.
24) Arber DA, Stein AS, Carter NH, Ikle D, Forman SJ, Slovak ML. Prognostic impact of acute myeloid leukemia classification. Importance of detection of recurring cytogenetic abnormalities and multilineage dysplasia on survival. Am J Clin Pathol. 2003; **119**: 672-680.
25) Fenaux P, Mufti GJ, Hellstrom-Lindberg E, et al. Efficacy of azacitidine compared with that of conventional care regimens in the treatment of higher-risk myelodysplastic syndromes: a randomised, open-label, phase III study. Lancet Oncol. 2009; **10**: 223-232.
26) Kantarjian H, O'Brien S, Ravandi F, et al. Proposal for a new risk model in myelodysplastic syndrome that accounts for events not considered in the original International Prognostic Scoring System. Cancer. 2008; **113**: 1351-1361.
27) Sanada M, Suzuki T, Shih LY, et al. Gain-of-function of mutated C-CBL tumour suppressor in myeloid neoplasms. Nature. 2009; **460**: 904-908.
28) Elghetany MT. Surface marker abnormalities in myelodysplastic syndromes. Haematologica. 1998; **83**: 1104-1115.
29) Wells DA, Benesch M, Loken MR, et al. Myeloid and monocytic dyspoiesis as determined by flow cytometric scoring in myelodysplastic syndrome correlates with the IPSS and with outcome after hematopoietic stem cell transplantation. Blood. 2003; **102**: 394-403.
30) van de Loosdrecht AA, Westers TM, Westra AH, et al. Identification of distinct prognostic subgroups in low- and intermediate-1-risk myelodysplastic syndromes by flow cytometry. Blood. 2008; **111**: 1067-1077.
31) Ogata K, Kishikawa Y, Satoh C, Tamura H, Dan K, Hayashi A. Diagnostic application of flow cytometric characteristics of CD34+ cells in low-grade myelodysplastic syndromes. Blood. 2006; **108**: 1037-1044.
32) van de Loosdrecht AA, Alhan C, Béné MC, et al. Standardization of flow cytometry in myelodysplastic syndromes: report from the first European LeukemiaNet working conference on flow cytometry in myelodysplastic syndromes. Haematologica. 2009; **94**: 1124-1134.
33) Heinrichs S, Kulkarni RV, Bueso-Ramos CE, et al. Accurate detection of uniparental disomy and microdeletions by SNP array analysis in myelodysplastic syndromes with normal cytogenetics. Leukemia. 2009; **23**: 1605-1613.
34) Harada H, Harada Y, Tanaka H, Kimura A, Inaba T. Implications of somatic mutations in the AML1 gene in radiation-associated and therapy-related myelodysplastic syndrome/acute myeloid leukemia. Blood. 2003; **101**: 673-680.
35) O'Keefe C, McDevitt MA, Maciejewski JP. Copy neutral loss of heterozygosity: a novel chromosomal lesion in myeloid malignancies. Blood. 115: 2731-2739.
36) Langemeijer SM, Kuiper RP, Berends M, et al. Acquired mutations in TET2 are common in myelodysplastic syndromes. Nat Genet. 2009; **41**: 838-842.
37. Kosmider O, Gelsi-Boyer V, Cheok M, et al. TET2 mutation is an independent favorable prognostic factor in myelodysplastic syndromes (MDSs). Blood. 2009; **114**: 3285-3291.
38) Mardis ER, Ding L, Dooling DJ, et al. Recurring mutations found by sequencing an acute myeloid leukemia genome. N Engl J Med. 2009; **361**: 1058-1066.

Aberrant induction of LMO2 by the E2A-HLF chimeric transcription factor and its implication in leukemogenesis of B-precursor ALL with t(17;19)

Kinuko Hirose,[1] Takeshi Inukai,[1] Jiro Kikuchi,[2] Yusuke Furukawa,[2] Tomokatsu Ikawa,[3] Hiroshi Kawamoto,[3] S. Helen Oram,[4] Berthold Göttgens,[4] Nobutaka Kiyokawa,[5] Yoshitaka Miyagawa,[5] Hajime Okita,[5] Koshi Akahane,[1] Xiaochun Zhang,[1] Itaru Kuroda,[1] Hiroko Honna,[1] Keiko Kagami,[1] Kumiko Goi,[1] Hidemitsu Kurosawa,[6] A. Thomas Look,[7] Hirotaka Matsui,[8] Toshiya Inaba,[8] and Kanji Sugita[1]

[1]Pediatrics, School of Medicine, University of Yamanashi, Yamanashi, Japan; [2]Stem Cell Regulation, Center for Molecular Medicine, Jichi Medical School, Tochigi, Japan; [3]Laboratory for Lymphocyte Development, RIKEN Research Center for Allergy and Immunology, Yokohama, Japan; [4]Department of Haematology, Cambridge Institute for Medical Research, Cambridge University, Cambridge, United Kingdom; [5]Developmental Biology, National Research Institute for Child Health and Development, Tokyo, Japan; [6]Department of Pediatrics, Dokkyo Medical School, Tochigi, Japan; [7]Pediatric Oncology, Dana-Farber Cancer Institute, Boston, MA; and [8]Molecular Oncology, Research Institute for Radiation Biology and Medicine, Hiroshima University, Hiroshima, Japan

LMO2, a critical transcription regulator of hematopoiesis, is involved in human T-cell leukemia. The binding site of proline and acidic amino acid–rich protein (PAR) transcription factors in the promoter of the *LMO2* gene plays a central role in hematopoietic-specific expression. E2A-HLF fusion derived from t(17;19) in B-precursor acute lymphoblastic leukemia (ALL) has the transactivation domain of E2A and the basic region/leucine zipper domain of HLF, which is a PAR transcription factor, raising the possibility that E2A-HLF aberrantly induces LMO2 expression. We here demonstrate that cell lines and a primary sample of t(17;19)-ALL expressed LMO2 at significantly higher levels than other B-precursor ALLs did. Transfection of *E2A-HLF* into a non-t(17;19) B-precursor ALL cell line induced *LMO2* gene expression that was dependent on the DNA-binding and transactivation activities of E2A-HLF. The PAR site in the *LMO2* gene promoter was critical for E2A-HLF-induced LMO2 expression. Gene silencing of *LMO2* in a t(17;19)-ALL cell line by short hairpin RNA induced apoptotic cell death. These observations indicated that E2A-HLF promotes cell survival of t(17;19)-ALL cells by aberrantly up-regulating LMO2 expression. LMO2 could be a target for a new therapeutic modality for extremely chemo-resistant t(17;19)-ALL. (*Blood*. 2010;116(6):962-970)

Introduction

Transcription factors that regulate normal hematopoiesis are frequently involved in leukemogenesis[1,2] through 2 types of chromosomal translocation: one causes in-frame fusion of 2 genes and the resultant chimeric transcription factor acquires novel functions and/or functionally disrupts the normal gene products, and the other causes aberrant activation of a transcription factor gene due to juxtaposition to a strong enhancer of the immunoglobulin or T-cell receptor (TCR) loci. The *LMO2* gene, located on the short arm of chromosome 11 at band 13 (11p13), was discovered from a recurrent site of translocations in T-cell acute lymphoblastic leukemia (T-ALL) as a paradigm of the latter type of translocation.[3,4] LMO2 is a member of the LIM-only zinc finger protein family and is present in a transcription factor complex[5] that also includes E2A, TAL1, GATA1, and LDB1 in erythroid cells.[6] Within this complex, LMO2 mediates the protein-protein interactions by recruiting LDB1,[7] whereas TAL1, GATA1, and E2A directly bind to the specific DNA target sites.[6,8] Homozygous null mutation of *Lmo2* showed embryonic lethality due to lack of yolk sac erythropoiesis,[9] and chimeric animals produced from homozygous-deficient embryonic stem cells demonstrated a requirement of *Lmo2* in adult hematopoiesis[10] and angiogenic remodeling of the vasculature.[11] *Lmo2* is expressed in long-term repopulating hematopoietic stem cells[12] and in hematopoietic progenitors,[9] and its expression is maintained in erythroid cells during differentiation. In contrast, *Lmo2* expression is repressed in terminally differentiated granulocytes, macrophages, T cells, and B cells[9] with the exception of germinal center B cells.[13-15] During T-cell development, *Lmo2* is expressed in immature CD4/CD8 double-negative thymocytes and is down-regulated as maturation progresses,[16] and transgenic mice expressing *Lmo2* using a thymocyte-specific promoter developed an accumulation of CD4/CD8 double-negative thymocytes and eventually a T-cell lymphoma.[17-20] Of note, among X-linked severe combined immunodeficiency patients receiving retroviral *IL2Rγc* gene therapy, 2 patients developed T-ALL due to aberrant activation of *LMO2* via integration of the retroviral vector in the *LMO2* gene.[16,21,22] These observations suggested that deregulated *LMO2* increases susceptibility to T-cell malignancies by blocking differentiation. Although similar down-regulation of LMO2 was suggested during B-cell development,[9] the significance of LMO2 expression in B-precursor ALL remains totally unclarified.

The *LMO2* gene has 2 transcriptional promoters and comprises 6 exons, of which exons 4, 5, and 6 encode the protein.[23] The distal and proximal promoters are located upstream of exon 1 or 3 of the larger transcripts, respectively, and the 2 resultant transcripts encode the same open reading frame. The proximal promoter is active in hematopoietic progenitor and endothelial cells, dependent

Submitted September 21, 2009; accepted April 15, 2010. Prepublished online as *Blood* First Edition paper, June 2, 2010; DOI 10.1182/blood-2009-09-244673.

The online version of this article contains a data supplement.

The publication costs of this article were defrayed in part by page charge payment. Therefore, and solely to indicate this fact, this article is hereby marked "advertisement" in accordance with 18 USC section 1734.

on activation of 3 conserved Ets sites,[24] but transgenic analysis demonstrated that the proximal promoter alone is insufficient for full expression of the *Lmo2* gene in hematopoietic cells.[24] The distal promoter is involved in hematopoietic-specific *LMO2* gene expression that is dependent on activation of the proline and acidic amino acid-rich protein (PAR) site in the *LMO2* gene promoter.[25] The PAR transcription factors belong to the basic region/leucine zipper (bZIP) factor family and include hepatic leukemic factor (HLF),[26,27] albumin gene promoter D-site binding protein (DBP),[28] and thyrotroph embryonic factor (TEF).[29] Among the PAR transcription factors, it has been demonstrated that TEF shows the highest potential to activate the *LMO2* promoter in erythroid cells.[25]

t(17;19)(q21-q22;p13) is a relatively rare translocation among childhood ALL cases[2] and is linked with the B-precursor phenotype. E2A-HLF derived from t(17;19) promotes anchorage-independent growth of murine fibroblasts[30,31] and protects cells from apoptosis induced by growth factor deprivation,[32-34] and *E2A-HLF* transgenic mice develop T-cell malignancies.[35,36] In E2A-HLF chimera, the transactivation domain of E2A fuses to the bZIP dimerization and DNA-binding domain of HLF, one of the PAR transcription factors.[26,27] As a result, E2A-HLF recognizes the consensus sequence of PAR transcription factors as a dimer and transactivates downstream target genes.[27,31,37,38] Considering the critical involvement of the PAR site in the distal promoter of the *LMO2* gene in the hematopoietic-specific expression of *LMO2*,[25] E2A-HLF might induce aberrant expression of *LMO2* through the distal promoter. In the present study, we show aberrantly higher expression of LMO2 in t(17;19)-ALL as one of the direct targets of E2A-HLF. The biologic significance of LMO2 in leukemogenesis of t(17;19)-ALL is also investigated and discussed.

Methods

Leukemia cell lines and patient sample

Four ALL cell lines with 17;19 translocation (UOC-B1, HALO1, YCUB2, Endo-kun) were used in this study. As B-precursor ALL cell lines, 9 *MLL*-rearranged ALL cell lines (KOPN-1, KOPB-26, KOCL-33, -44, -45, -50, -51, -58, and -69),[39] 6 Philadelphia chromosome (Ph1)–positive ALL cell lines (KOPN-30bi, -57bi, -66bi, -72bi, YAMN-73, and -91),[40] 7 t(1;19)-ALL cell lines (697, KOPN-34, -36, -60, -63, YAMN-90, and -92), and 6 other ALL cell lines including 1 with t(12;21) (Reh) and 5 with others (KOPN-35, -61, -62, -79, and -84) were used. Seven T-ALL cell lines (KOPT-K1, -5, -6, -11, YAMT-12, Jurkat, and MOLT4F), 4 Burkitt B-cell lines (KOBK-130, Daudi, Namalwa, and Raji), and 4 Epstein-Barr virus (EBV)–transformed normal B-cell lines (YAMB-1, -3, -4, and -9) were also used. All cell lines were maintained in RPMI1640 medium supplemented with 10% fetal calf serum (FCS) in a humidified atmosphere of 5% CO_2 at 37°C. Analysis of a sample from a patient with t(17;19)-ALL was approved by the Ethical Review Board of the University of Yamanashi. Mononuclear cells (blasts > 95%) that had been isolated from bone marrow aspirates of the patient by Ficoll-Hypaque density centrifugation were stored in liquid nitrogen with 15% dimethyl sulfoxide in fetal calf serum (FCS).

Isolation of normal B precursors

The $CD34^+$ population was separated from human cord blood mononuclear cells (MNCs) using MACS MicroBeads (Miltenyi Biotec) and, subsequently, $CD34^+/CD19^-$ and $CD34^+/CD19^+$ populations were sorted by flow cytometry (FACS Vantage; Becton Dickinson) using FITC-Lineage marker (CD3, CD4, CD8, CD11b, CD56, CD235a, CD41a) in combination with PE-CD34 and APC-CD19. $CD19^+/IgM^-$ and $CD19^+/IgM^+$ populations were sorted from human cord blood MNCs by flow cytometry using FITC-Lineage marker in combination with PE-IgM and APC-CD19. The $CD19^+$ population was also directly separated from peripheral blood MNCs with MACS MicroBeads. RNA was extracted from each population using RNeasy mini kit (QIAGEN), and cDNA was synthesized using SuperScript VILO cDNA synthesis kit (Invitrogen).

Western blot analysis

Cells were solubilized in Nonidet P-40 lysis buffer, and total cellular proteins were separated by sodium dodecyl sulfate–polyacrylamide gel electrophoresis (SDS-PAGE) under reducing conditions. After transfer onto nitrocellulose membrane and blocking with 5% nonfat dry milk in 0.05% Tween-20 Tris [tris(hydroxymethyl)aminomethane]–buffered saline (TBS), the membrane was incubated with the primary antibodies in 5% milk in TBS. Goat anti–human LMO2 and mouse anti–human α-Tubulin antibodies were purchased from R&D Systems and Sigma-Aldrich, respectively. Rabbit anti–human antibodies against E2A and HLF(C) were established as previously reported.[37] Membranes were incubated with horseradish peroxidase–conjugated rabbit anti–goat, goat anti–mouse, and goat anti–rabbit IgG (1:1000 dilution; MBL) and were then developed using the enhanced chemiluminescence kit (Amersham Pharmacia Biotech).

Real-time PCR analysis

Total RNA was extracted using Trizol reagent (Invitrogen). Reverse transcription (RT) was performed using random hexamer (Amersham Bioscience) by Superscript II reverse transcriptase (Invitrogen), and then the cDNA product was incubated with RNase (Invitrogen). For quantitative real-time polymerase chain reaction (PCR) of *LMO2*, triplicated samples containing cDNA with Taqman Universal PCR Master Mix (Applied Biosystems) and Gene Expression Product (exons 1/2, HS00951959_m1; exons 4/5, HS00277106_m1; Applied Biosystems) were amplified according to the manufacturer's protocol using KOPT-6 derived from T-ALL with t(11;14) as a control. As an internal control for relative gene expression, quantitative real-time PCR for *GAPDH* (Hs 99999905_m1, Applied Biosystems) was performed.

Semiquantitative PCR of transcripts derived from distal and proximal promoters

RNA transcripts originating from the distal *LMO2* promoter were quantified with forward primer 5′-CAAAGCAGGCAATTAGCCC-3′ and reverse primer 5′-CCTCTCCACTAGCTACTGC-3′, which are situated in exons 1 and 2, respectively. Total *LMO2* expression was quantified with forward primer 5′- GAGCTGCGACCTCTGTGG-3′ and reverse primer 5′-CACCCGCATTGTCATCTCAT-3′, which are situated in exons 5 and 6, respectively. Standard curves were created against a single copy of the *LMO2* full-length cDNA subcloned into the pGEMT Easy (Promega) backbone. The assay was performed in triplicate, and the mean quantity of proximal promoter-derived transcripts was directly calculated by subtracting the mean quantity of distal promoter-derived transcripts from the mean quantity of total transcripts. To consider the degree of approximation of the calculated mean, the following equation was considered: var(a+b) = var(a)+var(b)+2cov(a,b). The standard deviation of the quantity of proximal promoter-derived transcripts is therefore assumed to be represented as follows: SD prox LMO2 = sqrt [(SD total LMO2)^2- (SD distal LMO2)^2].

Construction of eukaryotic expression vectors and transfection

Expression plasmids containing wild-type and mutated *E2A-HLF* cDNA were constructed with the pMT-$CB6^+$ eukaryotic expression vector (a gift from F. Rauscher III, Wistar Institute, Philadelphia, PA),[32] which contains the inserted cDNA under control of a sheep metallothionein promoter. ΔAD1/ΔLH mutant and Basic region mutant (BX) were prepared as previously reported.[30,33] Transfectants were generated by electroporation followed by selection using neomycin analog G418 as previously reported.[33]

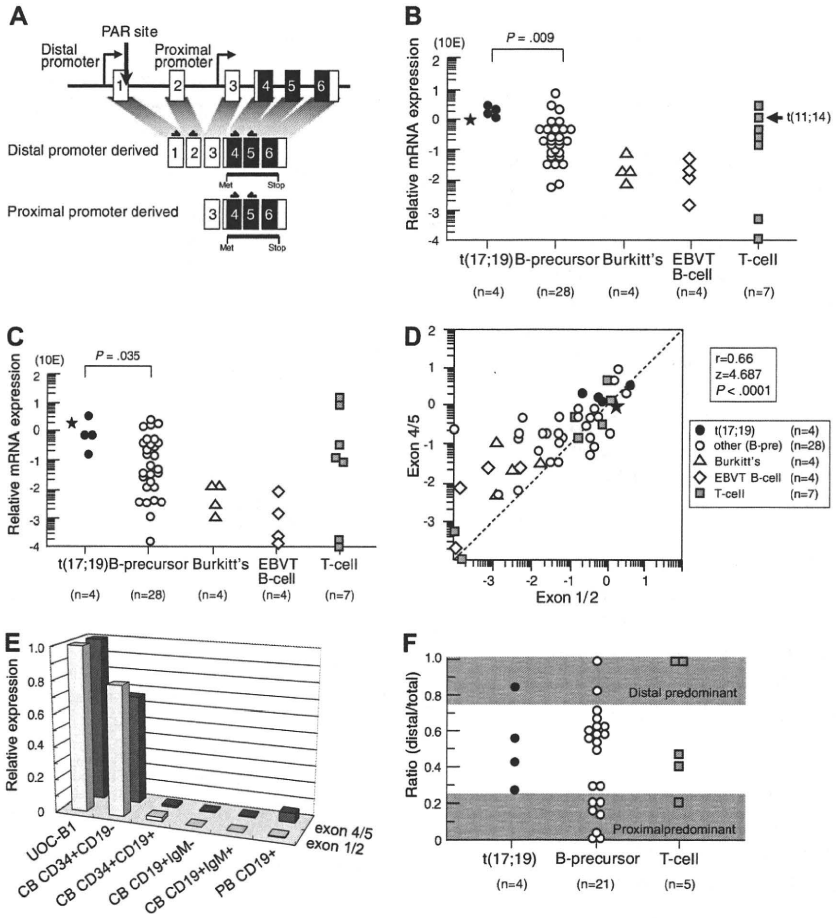

Figure 1. LMO2 gene expression in t(17;19)-ALL. (A) Schematic representation of 2 *LMO2* gene promoters and primers for real-time RT-PCR analysis. Primers directed toward exons 1 and 2 specifically detect transcripts derived from the distal promoter, and those directed toward exons 4 and 5 detect transcripts derived from both the distal and proximal promoters. (B) Relative *LMO2* gene expression determined by real-time RT-PCR using the primers for exons 4 and 5. Arrow indicates T-ALL cell line with t(11;14), and asterisk indicates the level of *LMO2* transcripts in a primary leukemia sample from the patient with t(17;19)-ALL. The *P* value determined by Mann-Whitney test is indicated. (C) Relative *LMO2* gene expression determined by real-time RT-PCR using the primers for exons 1 and 2. (D) Correlation between the levels of *LMO2* transcripts quantified by the primers for exons 4 and 5 (vertical axis) and those for exons 1 and 2 (horizontal axis). (E) *LMO2* gene expression in $CD34^+/CD19^-$, $CD34^+/CD19^+$, $CD19^+/IgM^-$, and $CD19^+/IgM^+$ populations of cord blood mononuclear cells (MNCs) and $CD19^+$ population of peripheral blood MNCs. Relative *LMO2* gene expression was determined by real-time RT-PCR using UOC-B1 as a control with the primers for exons 1 and 2 and the primers for exons 4 and 5. The gene expression level of *β-actin* was used as an internal control. SE of triplicated samples was always less than 10%. (F) Ratio of *LMO2* gene expression derived from the distal promoter to total *LMO2* gene expression in ALL cell lines. *LMO2* gene expression in the cell lines that expressed a total *LMO2* gene level of at least 10 times lower than that in UOC-B1 was semiquantifiedby real-time PCR with the specific primers for *LMO2* transcripts sourced at the distal promoter and for total *LMO2* transcripts. The dark areas indicate a proximal promoter-predominant pattern (ratio < 0.25) or a distal promoter-predominant pattern (ratio > 0.75).

Electrophoretic mobility shift assay

Nuclear extracts of cells were prepared and binding reactions were performed as previously reported.[31,37] Briefly, a ^{32}P-end-labeled oligonucleotide probe containing wild-type HLF consensus sequence (CS; 5′-GCTACAT*ATTACGTAAT*AAGCGTT-3′) was incubated in 10 μL of binding buffer and 5 μL of nuclear lysates in the presence of 1 μg of shared calf thymus DNA. In the competition inhibition experiments, an approximately 100-fold molar excess of the unlabeled oligonucleotide was added to the reaction mixture. Polyvalent HLF(C) or E2A rabbit antiserum was added to the nuclear lysates before the DNA-binding reaction.

Reporter assays

−512/+428 *Kpn*I-*Hin*dIII fragment and −512/+249 *KpnI*/*Bgl*II fragment of the *LMO2* gene generated by PCR were cloned into the pGL3 basic vector (Promega). −512/+428 PAR^M that has the sequence *CATCG*ATCAT instead of ATTACATCAT in the PAR site was generated by PCR mutagenesis. All constructs were subjected to nucleotide sequence analysis to verify the appropriate insertions. pGL3 control vector and pRL-TK vector were used as the positive control and internal control of transfection efficiency, respectively. For transfection, wild type and E2A-HLF-expressing Nalm6 cells were plated at 5×10^5 cells/well in a 24-well plate and a total of 5 μg of luciferase reporter plasmid, 1 μg of pRL-TK and 2 μL of lipofectamine (Invitrogen) in 50 μL of serum-free medium (Opti-MEM I; Invirogen) were added. After 24 hours of culture, 100μM $ZnSO_4$ at final concentration was added to induce E2A-HLF expression. Cells were harvested 48 hours after transfection and lysed in 50 μL of lysis buffer (Promega). Activities of firefly and *Renilla* luciferases in each lysate were measured sequentially using the Dual-Luciferase reporter assay system from Promega by a luminometer according to the manufacturer's instructions.

Lentivirus shRNA/siRNA expression vectors and infection

pLL3.7 lentiviral vector was engineered to produce short hairpin RNAs (shRNAs) under the control of mouse U6 promoter and co-express green fluorescent protein (GFP) as a reporter gene by cytomegalovirus-derived promoter–GFP expression cassette.[41] Short interfering RNA (siRNA) target sequences were designed to be homologous to the wild-type *LMO2* cDNA sequence, and oligonucleotides were subcloned into pLL3.7.[42] The selected sequences were submitted to BLAST search to assure that only *LMO2* was targeted. Among 5 sets of oligonucleotides containing siRNA target sequences, the following set was selected for further analysis due to the specificity and efficiency: 5′-Tgacgcatttcggttgagaa*TTCAAGAGA*Attctcaaccgaaatgcgtc*TTTTTTC*-3′(Blunt-siRNA/sense hairpin-siRNA/antisense-polyA-*Xho*I/forward);5′-TCGAGAAAAAAgacgcatttcggttgagaaTCTCTTGAAttctcaaccgaaatgcgtcA-3′(reverse). The control vector contained the following as ineffective set: 5′-Tgcaatattacatatacgcc*TTCAAGAGA*ggcgtatatgtaatattgc*TTTTTTC*-3′ (forward); 5′-TCGAGAAAAAAgcaatattacatatacgccTCTCTTGAAggcgtatatgtaatattgcA-3′(reverse). pLL3.7 shRNA vector or control vector was cotransfected with packaging vector into 293FT cells and the resulting supernatant was collected after 36 hours.[42] Lentivirus was recovered after ultracentrifugation and infected to UOC-B1 cells.

Results

Aberrant expression of LMO2 in t(17;19)-ALL

We first analyzed *LMO2* gene expression in 4 t(17;19)-ALL cell lines, UOC-B1, HALO1, YCUB2, and Endo-kun, by real-time RT-PCR using 2 different sets of primers (Figure 1A): one set

directed toward exons 1 and 2 that is specific for the transcripts derived from the distal promoter, and the other set directed toward exons 4 and 5 that is specific for the transcripts derived from both the distal and proximal promoters. Real-time RT-PCR analysis using the primers specific for exons 4 and 5 demonstrated that all 4 t(17;19)-ALL cell lines expressed *LMO2* transcripts at an equivalent level to that in KOPT6, a T-ALL cell line that aberrantly expresses LMO2 as a result of t(11;14) (Figure 1B). The level of *LMO2* transcripts in t(17;19)-ALL cell lines was significantly higher than that in 28 other B-precursor ALL cell lines ($P = .009$, Mann-Whitney test) including Ph1-ALL, t(1;19)-ALL, and *MLL*+ALL (supplemental Figure 1A, available on the *Blood* Web site; see the Supplemental Materials link at the top of the online article). Real-time RT-PCR analysis using the primers specific for exons 1 and 2 demonstrated that the level of *LMO2* transcripts derived from the distal promoter in t(17;19)-ALL cell lines was also significantly higher than that in the other B-precursor ALL cell lines (Figure 1C and supplemental Figure 1B). A strong correlation was observed between the levels of *LMO2* transcripts quantified by the 2 sets of primers among the 47 cell lines ($r = 0.66$, $P < .0001$; Figure 1D). The primary sample from a t(17;19)-ALL patient also demonstrated high levels of *LMO2* transcripts (Figure 1B-C). Consistent with down-regulation of *LMO2* gene expression during the progression of normal B-cell development,[9] the gene expression level of *LMO2* in Burkitt B-cell lines as well as EBV-transformed normal B-cell lines was unanimously low. Thus, the *LMO2* gene expression level during B-cell development was analyzed using fractions of cord blood and peripheral blood MNCs (Figure 1E). The *LMO2* gene expression level in the $CD34^+/CD19^-$ population of cord blood MNCs was almost equivalent to that in UOC-B1, and it was markedly down-regulated in the $CD34^+/CD19^+$ population. This low expression level was sustained in the $CD19^+/IgM^-$ and the $CD19^+/IgM^+$ populations of cord blood MNCs as well as in the $CD19^+$ population of peripheral blood MNCs.

Next, the contribution of the distal promoter was analyzed in those cell lines that expressed the total *LMO2* gene at a level of at least 10 times lower than that in UOC-B1 by real-time PCR using standard curves, which were created against DNA template of the full-length *LMO2* cDNA that was subcloned into the vector as a single copy. The ratio of the quantity of *LMO2* transcripts sourced at the distal promoter to the quantity of total *LMO2* transcripts in the t(17;19)-ALL cell lines was 0.26 to 0.83 (Figure 1F), indicating that both the distal and the proximal promoters contributed to *LMO2* gene expression. None of the 4 t(17;19)-ALL cell lines showed a proximal promoter-predominant pattern (ratio < 0.25), while 7 of 21 other B-precursor ALL cell lines and 1 of 5 T-ALL cell lines showed a proximal promoter-predominant pattern.

We next analyzed LMO2 protein expression by Western blotting using α-tubulin expression as an internal control. Consistent with the gene expression level, LMO2 protein was aberrantly expressed in all 4 t(17;19)-ALL cell lines at a similarly high level to that in the T-ALL cell line with t(11;14) (Figure 2A). compared with other B-precursor ALL cell lines (Figure 2B), the t(17;19)-ALL cell lines expressed significantly higher levels of LMO2 protein ($P = .005$, Mann-Whitney test). Consistent with the low gene expression level, protein expression of LMO2 was undetectable in both Burkitt B-cell lines and EBV-transformed normal B-cell lines. Strong correlations were observed between the levels of LMO2 protein and *LMO2* transcripts analyzed by the primers specific for exons 4 and 5 ($r = 0.72$, $P < .0001$, Figure 2C) and those for exons 1 and 2 ($r = 0.42$, $P = .0089$). These observations indicated that t(17;19)-ALL cells aberrantly express LMO2.

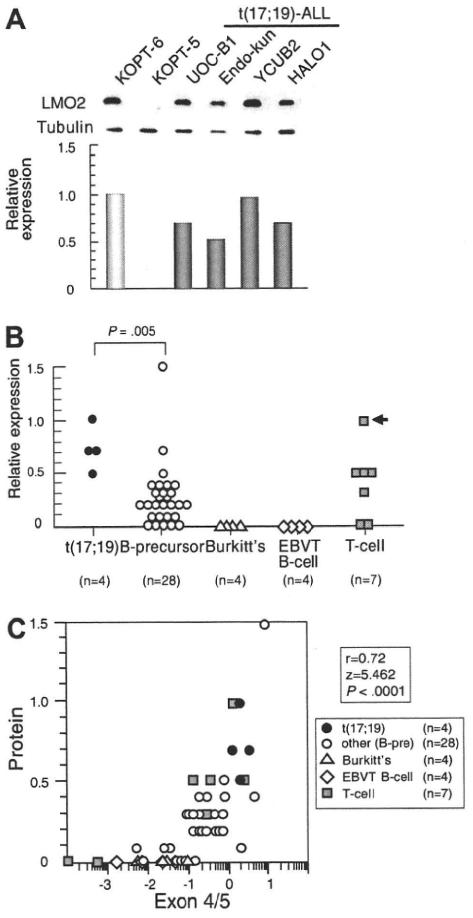

Figure 2. LMO2 protein expression in t(17;19)-ALL. (A) Western blot analysis of LMO2. Relative expression of each cell line was determined by quantifying the intensity of each band using KOPT6, a T-ALL cell line with t(11;14), as a positive control and KOPT-5, a T-ALL cell line without LMO2 expression, as a negative control, and normalized by the level of α-tubulin expression as an internal control. (B) Relative level of LMO2 protein expression. The *P* value determined by Mann-Whitney test is indicated. (C) Correlation between levels of relative protein expression of LMO2 (vertical axis) and gene expression of *LMO2* analyzed by real-time RT-PCR using the primers for exons 4 and 5 (horizontal axis).

Up-regulation of the *LMO2* gene expression by E2A-HLF

To test the possibility that aberrant expression of *LMO2* in t(17;19)-ALL cells is driven by E2A-HLF, we transfected *E2A-HLF* into B-precursor ALL cell line 697, which has t(1;19) and expresses approximately 100-fold lower level of *LMO2* gene than the t(17;19)-ALL cell lines, using a zinc-inducible vector. In E2A-HLF-transfected 697 cells, E2A-HLF was up-regulated to a level equivalent to that in UOC-B1 cells within 4 hours of the addition of zinc to the culture medium (Figure 3A). When analyzed by real-time RT-PCR using primers specific for exons 4 and 5 (Figure 3B), *LMO2* gene expression was up-regulated by the addition of zinc in the E2A-HLF-transfected 697 cells but not in the wild-type 697 cells. When the *LMO2* gene expression derived from the distal and the proximal promoters was differentially semiquantified by real-time PCR (Figure 3C), significant gene expression derived from the distal promoter was immediately induced within 4 hours after the addition of zinc. Subsequently, significant gene expression derived from the proximal promoter was induced within

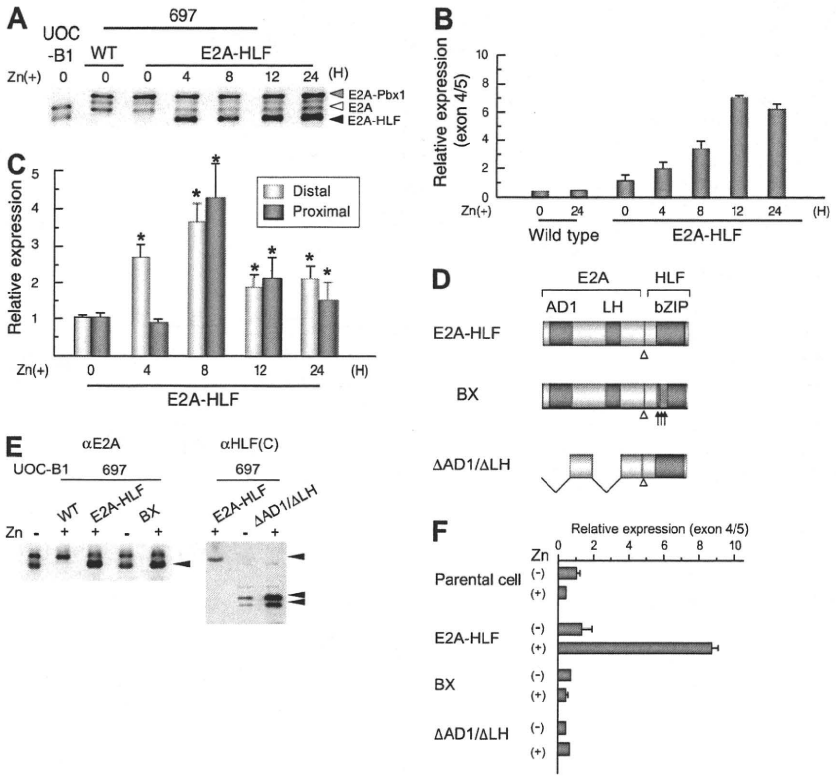

Figure 3. Induction of *LMO2* gene expression by E2A-HLF. (A) Induction of E2A-HLF expression. Lysates of wild type (WT) and a clone of *E2A-HLF*–transfected 697 cells as well as UOC-B1 cells harvested at the indicated time after the addition of zinc were blotted with an anti-E2A serum. Gray, white, and black arrowheads indicate E2A-Pbx1, E2A, and E2A-HLF, respectively. (B) Time course analysis of *LOM2* gene expression after induction of E2A-HLF. Levels of *LMO2* transcripts were quantified by real-time RT-PCR using the primers for exons 4 and 5, normalized by *GAPDH* gene expression as an internal control. Changes in fold induction of *LMO2* gene expression level to that in wild type 697 cells cultured in the absence of zinc are shown as the mean ± SE of triplicate samples. (C) Time course analysis of *LOM2* gene expression derived from the distal and proximal promoters after induction of E2A-HLF. Levels of *LMO2* transcripts in E2A-HLF–transfected 697 cells cultured in the presence of zinc were semiquantified by real-time RT-PCR with the specific primers for *LMO2* transcripts sourced at the distal promoter and for total *LMO2* transcripts. Changes in fold induction of *LMO2* gene expression level to that in E2A-HLF–transfected cells cultured in the absence of zinc are shown as the mean ± SE of triplicate samples. Asterisks indicate the significant gene induction determined by t-test. (D) Schematic diagram of mutants of E2A-HLF. (E) Western blot analysis of mutants of E2A-HLF. Lysates of UOC-B1 cells and wild-type (WT) and clones of 697 cells transfected with *E2A-HLF*, *BX*, and *ΔAD1/ΔLH* cultured in the absence or presence of zinc for 24 hours were blotted with E2A (left panel) and HLF(C) (right panel) antisera. (F) *LMO2* gene expression in mutant *E2A-HLF*–transfected 697 cells. Wild-type (WT) and transfectants of 697 cells were cultured in the absence or presence of zinc for 24 hours, and the levels of *LMO2* transcripts were quantified by real-time RT-PCR. Changes in fold induction of *LMO2* gene expression level to that in wild-type 697 cells cultured in the absence of zinc are shown as the mean ± SE of triplicate samples.

8 hours after the addition of zinc. These observations suggest that the distal and the proximal promoters of the *LMO2* gene sequentially contribute to E2A-HLF–induced *LMO2* gene expression. We further tested 2 types of E2A-HLF mutants in 697 cells. BX contains substitutions of 6 critical basic amino acids in the basic region of HLF to abolish DNA-binding ability, while ΔAD1/ΔLH lacks 2 transactivation domains of E2A to abolish transactivation ability but retain DNA-binding ability (Figure 3D).[30,33] Despite almost equivalent levels of expression of each mutant protein to that of E2A-HLF (Figure 3E), the gene expression level of *LMO2* remained unchanged after the addition of zinc (Figure 3F), indicating that both the DNA-binding and transactivation abilities of E2A-HLF are required for induction of *LMO2* gene expression.

Essential role of the PAR site in the distal promoter of the *LMO2* gene for up-regulation of *LMO2* expression by E2A-HLF

To determine whether E2A-HLF binds to the PAR site in the distal promoter of the *LMO2* gene, we performed electrophoretic mobility shift assay using HLF-CS sequence as a probe in the presence of the double-stranded oligomers listed in Figure 4A as competitors.[25] The DNA-protein complex of E2A-HLF, which was ablated or supershifted in the presence of anti-HLF(C) (Figure 4B lane 1) or anti-E2A (Figure 4B lane 2) antisera, respectively, was competed by the addition of oligomers centered on the PAR site in the distal promoter region (Figure 4B lanes 7-9), although less effectively than unlabeled HLF-CS probe (Figure 4B lanes 3-6). The oligomers containing 2-bp replacement in the 3′ region immediately outside of the PAR site (PAR^{TG}) effectively competed the formation of DNA-protein complex (Figure 4B lane 11), while those containing 2-bp (PAR^{CA}) or 4-bp (PAR^{M}) replacement within the PAR site (Figure 4B lanes 10,12) did not, indicating that the PAR site in the distal promoter of the *LMO2* gene is critical for the binding of E2A-HLF. We also performed electrophoretic mobility shift assay using the sequence of the PAR site in the distal promoter of the *LMO2* gene as a probe, but could not find significant binding (data not shown). High levels of sequence conservation among the mammalian sequences were reported across the entire *LMO2* genomic region.[24] The PAR site sequence in the distal promoter is highly conserved in chimpanzee (*Pan troglodytes*), cow (*Bos Taurus*), and mouse (*Mus musculus*; supplemental Figure 2A), suggesting that the PAR site plays an essential role in the *LMO2* gene expression in these mammalian species. Consistent with conservation of the PAR site in the distal promoter of mouse *lom2* gene, when *E2A-HLF* was transfected into FL5.12 cells, an IL-3–dependent mouse pro-B cell line, using zinc inducible vector as reported before,[33] *lmo2* gene expression derived from the distal

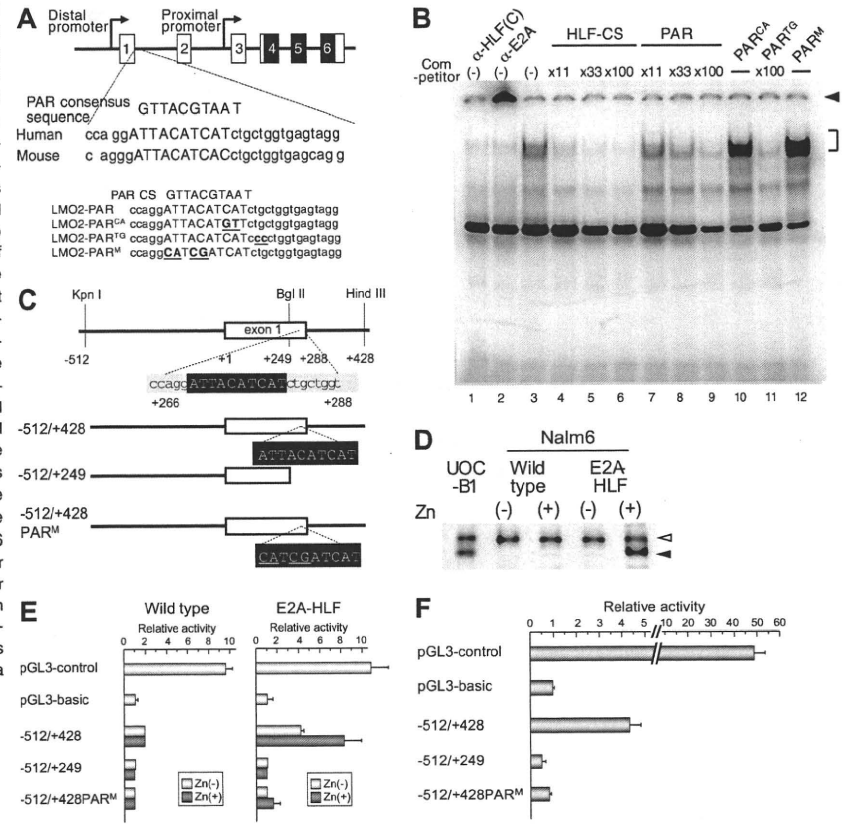

Figure 4. Involvement of the PAR site in the distal promoter of *LMO2* gene in E2A-HLF–induced LMO2 expression. (A) Schematic representation of the proline and acidic amino acid–rich protein (PAR) site in the distal promoter of the *LMO2* gene and oligonucleotides used as competitors in electrophoretic mobility shift assay. Mutations in the sequence are underlined. (B) Electrophoretic mobility shift assay performed in nuclear extracts from UOC-B1 cells using an HLF-CS sequence as a probe in the presence of a series of double-stranded oligomers as competitors (lanes 4-12) or anti-HLF(C) (lane 1) and anti-E2A (lane 2) sera. The molar ratio of cold competitor to probe is indicated in each lane. The specific DNA-protein complex is indicated by the bracket and the supershifted complex is indicated by the arrowhead. (C) Schematic representation of 3 reporter constructs for reporter assay. Mutations in the sequence are underlined. (D) Western blot analysis of E2A-HLF–transfected Nalm6 cells. Lysates of UOC-B1 cells and wild type and *E2A-HLF* transfected-Nalm6 cells cultured in the absence or presence of zinc for 24 hours were blotted with E2A antisera. Open and closed arrowheads indicate E2A and E2A-HLF, respectively. (E) Luciferase assay in E2A-HLF–transfected Nalm6 cells. Assays were performed in wild type and E2A-HLF–transfected Nalm6 cells cultured in the absence or presence of zinc for 24 hours after transient transfection of each reporter plasmid. The values were normalized for transfection efficiencies using a cotransfected *Renilla* luciferase construct. (F) Luciferase assay in YCUB2 cells. The values were normalized for transfection efficiencies using a cotransfected *Renilla* luciferase construct.

promoter was up-regulated by the addition of zinc in the *E2A-HLF*-transfected FL5.12 cells but not in the empty vector–transfected FL5.12 cells (supplemental Figure 2B).

We next performed luciferase assay of 3 reporter constructs[25] (Figure 4C) in Nalm6 cells transfected with *E2A-HLF* using a zinc-inducible vector. In E2A-HLF-transfected Nalm6 cells, E2A-HLF was faintly expressed in the absence of zinc, and it was up-regulated in the presence of zinc to a level equivalent to that in UOC-B1 cells (Figure 4D). When the −512/+428 reporter construct was transiently transfected, transcriptional activity was up-regulated in E2A-HLF–transfected Nalm6 cells in the presence of zinc whereas it was virtually silent in the wild-type Nalm6 cells (Figure 4E). Transcriptional activity of the distal promoter was completely abolished by deletion or mutation of the PAR site. Exactly the same pattern of promoter activities was verified in YCUB2, one of the t(17;19)-ALL cell lines (Figure 4F), demonstrating that E2A-HLF up-regulates *LMO2* gene expression by binding to the PAR site in the distal promoter of the *LMO2* gene.

Induction of apoptosis by shRNA for *LMO2* in a t(17;19)-ALL cell line

To study the significance of aberrant *LMO2* expression in leukemogenesis in t(17;19)-ALL, we introduced shRNA against *LMO2* into the t(17;19)-positive UOC-B1 cell line using a lentivirus vector, which contains *GFP* cDNA for cell sorting (Figure 5A).[41] The expression level of the *LMO2* gene in the GFP-positive (+) population of shRNA virus–infected UOC-B1 (shRNA/UOC-B1) cells was approximately 1000-fold lower than that in the GFP+ control virus–infected UOC-B1 (control/UOC-B1) cells when analyzed by real-time RT-PCR using the primers for exons 4 and 5 (Figure 5B). Despite infection with the same multiplicity of infection, the percentage of the GFP+ population decreased in the shRNA/UOC-B1 cells, in particular the GFP^{high} population that is supposed to express a higher level of shRNA, whereas it was unchanged in the control/UOC-B1 cells (Figure 5C). The percentage of the GFP+ population in shRNA/UOC-B1 cells was significantly lower than that in the control/UOC-B1 cells (Figure 5D, 7.5% vs 30.5% on day 5 after infection; $P = .003$ by t test). By contrast, when infected into 697 cells, a t(1;19)-ALL cell line used as a control, the percentage of the GFP+ population was stable in both the shRNA-virus-infected and the control virus-infected cells (Figure 5C).

To determine whether the reduction in the GFP+ cells in shRNA/UOC-B1 cells was due to cell death or cell-cycle arrest, we performed flow cytometric analysis of BrdU/7-AAD double staining on day 3 after infection (Figure 5E). The percentage of sub-G0/G1 apoptotic cells in the GFP+ shRNA/UOC-B1 cells was significantly higher than that in the control/UOC-B1 cells (12.4% vs 3.6%; $P = .014$ by t test, Figure 5F), while the percentages of cells in the G0/G1, S, and G2/M phases were almost unchanged. Moreover, as shown in Figure 5G, the percentage of caspase-3–activated cells in the GFP+ shRNA/UOC-B1 cells was significantly higher than that in the control/UOC-B1 cells (21.4% vs 0.5%; $P = .00087$ by t test). These observations demonstrate that induction of apoptotic cell death is responsible for the reduction in the GFP+ population among shRNA/UOC-B1 cells.

Discussion

In T-ALL, 2 mechanisms of aberrant expression of the *LMO2* gene have been well characterized: one is translocation of the *LMO2* gene, leading to its combination with enhancers or other regulatory elements of *TCR* genes,[1,3,4,43] and the other is cryptic deletion at

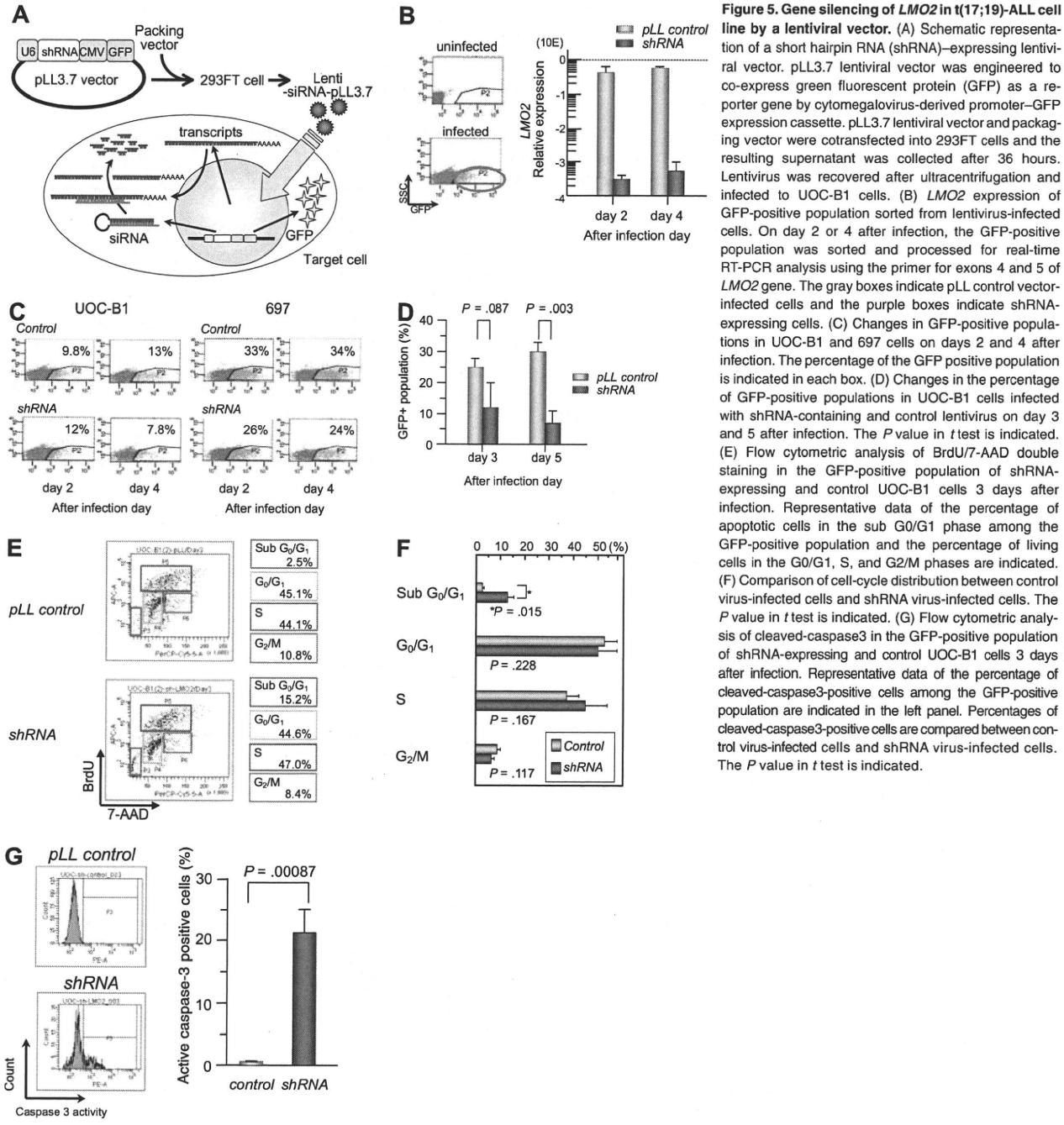

Figure 5. Gene silencing of *LMO2* in t(17;19)-ALL cell line by a lentiviral vector. (A) Schematic representation of a short hairpin RNA (shRNA)–expressing lentiviral vector. pLL3.7 lentiviral vector was engineered to co-express green fluorescent protein (GFP) as a reporter gene by cytomegalovirus-derived promoter–GFP expression cassette. pLL3.7 lentiviral vector and packaging vector were cotransfected into 293FT cells and the resulting supernatant was collected after 36 hours. Lentivirus was recovered after ultracentrifugation and infected to UOC-B1 cells. (B) *LMO2* expression of GFP-positive population sorted from lentivirus-infected cells. On day 2 or 4 after infection, the GFP-positive population was sorted and processed for real-time RT-PCR analysis using the primer for exons 4 and 5 of *LMO2* gene. The gray boxes indicate pLL control vector-infected cells and the purple boxes indicate shRNA-expressing cells. (C) Changes in GFP-positive populations in UOC-B1 and 697 cells on days 2 and 4 after infection. The percentage of the GFP positive population is indicated in each box. (D) Changes in the percentage of GFP-positive populations in UOC-B1 cells infected with shRNA-containing and control lentivirus on day 3 and 5 after infection. The *P* value in *t* test is indicated. (E) Flow cytometric analysis of BrdU/7-AAD double staining in the GFP-positive population of shRNA-expressing and control UOC-B1 cells 3 days after infection. Representative data of the percentage of apoptotic cells in the sub G0/G1 phase among the GFP-positive population and the percentage of living cells in the G0/G1, S, and G2/M phases are indicated. (F) Comparison of cell-cycle distribution between control virus-infected cells and shRNA virus-infected cells. The *P* value in *t* test is indicated. (G) Flow cytometric analysis of cleaved-caspase3 in the GFP-positive population of shRNA-expressing and control UOC-B1 cells 3 days after infection. Representative data of the percentage of cleaved-caspase3-positive cells among the GFP-positive population are indicated in the left panel. Percentages of cleaved-caspase3-positive cells are compared between control virus-infected cells and shRNA virus-infected cells. The *P* value in *t* test is indicated.

11p12-13 resulting in loss of negative regulatory sequences of the *LMO2* gene.[44] These 2 chromosomal abnormalities directly induce aberrant expression of the *LMO2* gene. Here we demonstrated a novel mechanism for aberrant expression of the *LMO2* gene as a downstream target of E2A-HLF fusion transcript derived from t(17;19) based on the following observations: all 4 t(17;19)-ALL cell lines studied and a patient's sample expressed a high level of *LMO2* gene transcript, and transfection of *E2A-HLF* into 697 cells induced gene expression of *LMO2* that was dependent on the transactivation and DNA-binding activities of E2A-HLF. E2A-HLF specifically bound to the PAR site in the distal promoter of the *LMO2* gene at least in vitro and enhanced promoter activity. Moreover, *LMO2* transcripts derived from both the proximal and distal promoters were expressed in t(17;19)-ALL cell lines. E2A-HLF rapidly induced *LMO2* gene expression originating from the distal promoter, and then induced *LMO2* gene expression derived from the proximal promoter, suggesting that E2A-HLF induces *LMO2* gene expression not only directly through the PAR site in the distal promoter but also indirectly through the proximal promoter.

It has been reported that LMO2 expression is down-regulated during T-cell development at the transition from immature CD4/CD8 double-negative thymocytes to more mature stages[16] and that enforced expression of *LMO2* in thymocytes blocks differentiation of CD4/CD8 double-negative thymocytes and induces T-cell malignancies.[17-20] In the present study, we confirmed that *LMO2* gene expression in both EBV-transformed normal B-cell lines and Burkitt B-cell lines was significantly lower than that in B-precursor ALL cell lines. In particular, LMO2 protein expression was almost